

PRELIMINARY INVESTIGATIONS ON ACTIVATION ANALYSIS

A- Thesis

submitted in partial fulfilment of  
the requirements for the degree of

Master of Science

at the

University of Manitoba

by

Kelvin Bramadat

April, 1954.



## PREFACE

The work described in this thesis was carried out at the University of Manitoba during the months April, 1953 to February, 1954.

The author wishes to express sincere thanks to the directors of the research project - Dr. G.M. Brownell of the Geology Department, and Dr. R.W. Pringle of the Physics Department, for their keen interest and advice.

The assistance of the Geological Survey of Canada, in providing funds for the purchase of the equipment, and for a research grant, is gratefully acknowledged.

## SUMMARY

When an element is bombarded with neutrons, one or more radioisotopes is formed. The radioisotopes are unstable, and return to stability by the emission of beta and gamma rays. The induced activity and the decay time are characteristic of each radioisotope; the intensity of the induced activity is proportional to the quantity of the element, and thus a method of identification and quantitative determination of elements is implied.

The following is a report on the preliminary investigations of effecting a qualitative and quantitative analysis of elements by using slow neutrons for activation, and a scintillation counter for detection.

## CONTENTS

|  | Page |
|--|------|
| Introduction.....                                  | 1    |
| Description of Apparatus.....                      | 18   |
| Preliminary Investigations.....                    | 31   |
| Activation of Certain Elements.....                | 35   |
| Aluminum.....                                      | 36   |
| Silicon.....                                       | 43   |
| Aluminum and Silicon.....                          | 47   |
| Silver.....  | 54   |
| Manganese.....                                     | 60   |
| Copper.....  | 67   |
| Magnesium.....                                     | 72   |
| Sandstones, Shales and Limestone.....              | 76   |
| Practical Applications of Activation Analysis..... | 93   |
| Conclusion.....                                    | 95   |
| References.....                                    | 98   |

## INTRODUCTION

Research in activation analysis has been carried out by Long (1), Eichholz, and Gaudin, Sentfle and Freyberger (2). These experimenters used Geiger Mueller counters and proportional counters. The scintillation counter, used as a detector, has a higher efficiency and is thus a much better detecting device. It has been used as a scintillation spectrometer in the study of ray spectra and in the study of neutron-capture radiation (3). In fact, a large number of papers have been written about the applications of scintillation spectroscopy (4,5), and the scintillation spectrometer soon may be the most important instrument as far as the nuclear physicist is concerned.

The use of the scintillation counter in activation analysis is a novel application. The following report is an investigation of the use of the scintillation spectrometer in making an analysis of certain elements by induced radiation. It is anticipated that this will have special applications to problems in geology and possibly to some phases of industry. It is also desired to determine, if possible, the limitations of this method. To fully appreciate its advantages, a brief

discussion of the scintillation spectrometer will be given.

The scintillation spectrometer consists of a scintillator, a photomultiplier, an amplifier, a discriminator and a recording device. Many kinds of scintillators have been used. The most common crystal scintillators are anthracene, stilbene, sodium iodide activated with thallium, and lithium iodide activated with tin. In the work to be described in the following pages, sodium iodide was used exclusively and this scintillator will be discussed in detail.

When  $\gamma$  rays strike the crystal, three interactions may take place, depending on the energy of the  $\gamma$  ray quantum. These are the well established  $\gamma$  ray interactions with matter, and are the 'photoelectric effect', the 'Compton effect', and the 'pair production effect'. Electrons which have been ejected from atoms by incident photons are called photoelectrons, and the process is known as the 'photoelectric effect'. The photoelectric effect is very small for photons of energy greater than a few mev. and depends on the atomic number of the absorbing element. Its cross section is proportional to  $Z^{4.7}$  (6).

After the electron has been ejected, low energy X rays, characteristic of the absorbing element, are produced.

These are absorbed and thus contributes to the total excitation of the crystal.

If the  $\gamma$  ray quantum is scattered at an angle  $\Theta$  away from its original direction, and the electron, which has been struck, recoils in a direction at an angle  $\phi$  to the trajectory of the primary photon, the process is called the 'Compton process'. The electron thus ejected, appears with an energy equal to that lost by the photon. The secondary photon however, has considerably less energy than the primary photon, and may be captured photoelectrically if the quantity of material through which it has to pass is appreciable. The Compton electrons have a continuous energy distribution. The cross section for the Compton effect is approximatedly proportional to  $Z(7)$ .

If a high energy  $\gamma$  ray (greater than 1.02 mev.) passes close to a nucleus, the  $\gamma$  ray may disappear completely, giving rise to two particles, an electron and a positron. This is the 'pair production process'. As its energy approaches zero, the positron eventually interacts with an electron and both disappear with the production of an annihilation quantum of energy 1.02 mev. Both electrons and positrons are produced with a continuous distribution, and the cross section for pair production is roughly proportional to  $Z^2(8)$ .

Since iodine<sup>138</sup> constitutes 85% of the NaI(Tl) crystal, nearly all the interactions would be  $\gamma$  ray-iodine<sup>138</sup> interactions. The relative cross section for the various interactions as a function of  $\gamma$  ray energy is shown in figure 1. It is clearly seen that the Compton and photoelectric effects are the predominant interactions for energies of  $\gamma$  ray less than 2 mev.

Gamma rays, striking a crystal, thus produce photons in the scintillator. These excite centres of fluorescence in the crystal lattice. The photomultiplier detects and amplifies these scintillations by a factor of about  $10^6$ . These electron spurts are converted into voltage pulses by a cathode follower, and these are transmitted to a linear amplifier. The pulse height distribution is then obtained from the discriminator. The relationship between the energy of the incident quantum and the pulse height is a linear one, and thus the energy of the incident  $\gamma$  ray can be determined directly from the shape of the pulse height distribution.

The main feature of activation analysis is the detection of the  $\gamma$  rays produced by the isotopes formed when the test sample is exposed to a source of thermal neutrons. In the discussion of the scintillation spectrometer, the existence of the  $\gamma$  ray quantum was presupposed. It is thus pertinent to discuss briefly the nuclear process which results in the production of the  $\gamma$  ray.



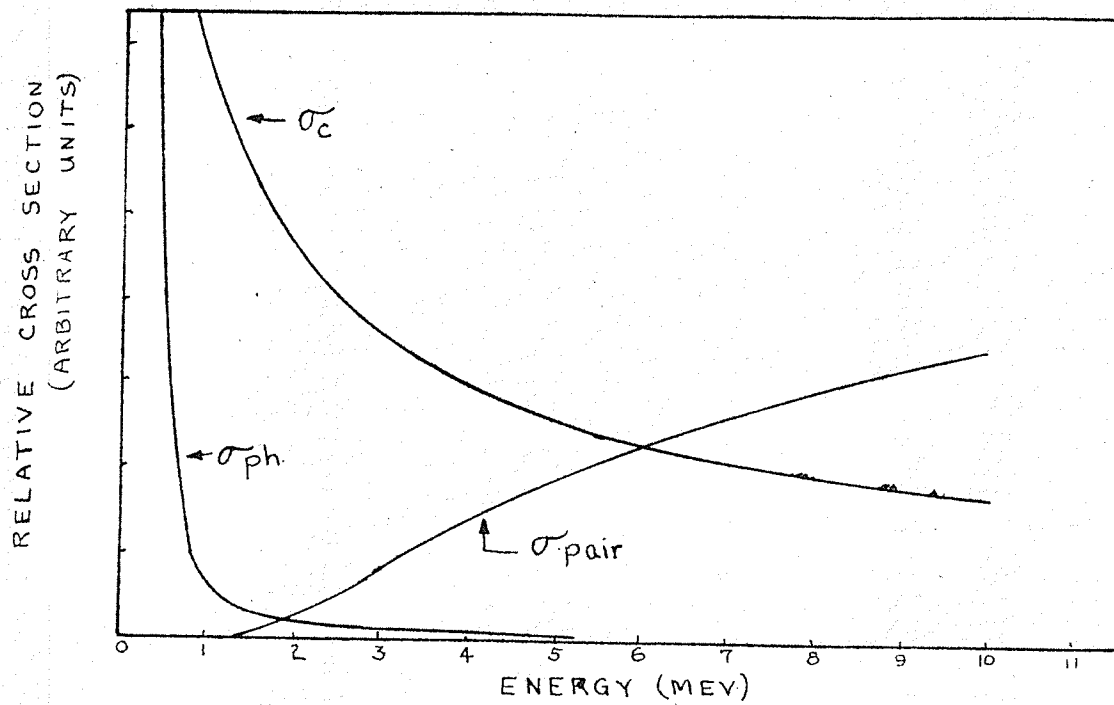


FIGURE [6]

RELATIVE CROSS SECTIONS FOR PHOTOELECTRIC (ph), COMPTON (c),  
AND PAIR PRODUCTION (pair) PROCESSES IN IODINE.

A nuclear reaction is a two step process (9). The first is the amalgamation of the incident particle, in this case a neutron, and the target nucleus to form a compound nucleus. The second step is the immediate disintegration of the excited nucleus to form the products of the reaction.

Using Bohr's concept that the nucleus is a densely packed bundle of nucleons, a neutron striking such a system would lose most of its kinetic energy in the first few collisions, and would then be held by the nuclear forces. Thus the compound nucleus is formed, and it possesses not only the kinetic energy of the neutron, but also the binding energy of the target nucleons. If the energy of the impinging neutron is very much smaller than the neutron energy at which the total excitation energy is equal to the energy difference between the energy level and the ground state of the compound nucleus, the compound nucleus can still be formed (10). It has been shown by Breit and Wigner (11) that the cross section for an  $(n, \gamma)$  reaction, using incident thermal neutrons ( $1/40$  ev.) is large.

The formation of a compound nucleus may result in a number of reactions. The competition between these reactions is usually described in terms of the 'reaction width', which is a measure of the probability (the inverse of the lifetime) for a given mode of disintegration of the compound nucleus. The value of the cross section for a particular reaction at a given neutron energy is determined by the proximity of this excitation energy to the energy values of one or more of the levels of the compound nucleus, and also by the relative values of the partial widths for the possible reactions.

The energy of the gamma radiation emitted by the compound nucleus depends on the energy of the initial configuration, as determined by the incident neutron energy, and on the energy of the ground state or intermediate state to which the transition occurs (12). The gamma ray energy will thus include the energy equivalent of the mass differences of the nuclei involved.

The compound nucleus in its excited state is usually very unstable, and decays exponentially to the stable products of disintegration. Analytically, the number ( $\Delta N$ ) of atoms disintegrating in a given time interval ( $\Delta t$ ) is proportional to the number ( $N$ ) of the radioactive atoms present.

(8)

$$\Delta N = \lambda N \Delta t \quad (1)$$

where  $\lambda$  is the decay constant.

$$\text{Integrating, } N = N_0 e^{-\lambda t} \quad (2)$$

$$\text{or log } \frac{(N_0)}{N} = 0.434 \lambda t \quad (3)$$

Where  $N_0$  is the total number of atoms present at  $t = 0$ .

This equation expresses the number of particles  $N$  that will exist at time  $t$ , if  $N_0$  radioactive atoms were present initially ( $t=0$ ). The half life,  $T$ , is the time required for a radioisotope to lose 50% of its activity, and a simple relationship exists between the disintegration or decay constant  $\lambda$ , and the half life. It is

$$\lambda = \frac{-\Delta N/N}{\Delta t} \quad (4)$$

For a given quantity of the radioelement, the activity might decrease very rapidly in a matter of seconds, or it may change more slowly over a period of years. The rate of change of activity is characteristic of the specific radioisotope under study.

The activity of any element irradiated in a beam of particles is given by the equation (13)

$$A = \frac{mF\epsilon}{M} (1 - e^{-0.7 T/t}) e^{-0.7t/T} \quad (5)$$

where  $m$  = mass of bombarded substance in grams.  
 $N$  = Avogadro's number ( $6.02 \times 10^{23}$  moles<sup>-1</sup>).  
 $M$  = Atomic weight of the element.  
 $F$  = bombarding flux per cm<sup>2</sup>. per sec.  
 $\epsilon$  = activation cross section, expressed in cm<sup>2</sup>.  
 $T$  = half life of active nucleus.  
 $t$  = time of irradiation.  
 $A$  = activity (ie) number of particles emitted per sec.

This equation shows that the activity of an element is directly proportional to the amount of the element used, the neutron flux available and the activation cross section for the reaction.

The cross sections for the  $(n, \gamma)$  reaction for the different elements vary from very small values (0.02 barns for tin,  $\text{Sn}^{118}$ ) to very large values (92 barns for silver,  $\text{Ag}^{109}$ ) (14). The isotopes formed have characteristic properties of initial activation, decay and half life, and  $\gamma$ -ray energies. If it is possible to determine these properties experimentally, then it should be possible to make a qualitative and quantitative analysis of a number of elements.

The importance of this method of analysis to geology is obvious, since the problem of rock analysis is very complex. This complexity is best shown by a review of 'petrology', or the science of rocks. The term 'rock' is used without reference to the hardness or state of cohesion of the material, and sands, shales, clays etc. are thus as much rocks in the scientific sense as granite or limestone.

The outer crust of the earth down to a depth of about ten miles consists of igneous rocks and metamorphic rocks with a thin interrupted mantle of sedimentary rocks resting on them. According to Clarke and Washington (15), the

percentage composition is : igneous rocks, 95%; shale, 4%; sandstone, 0.75%; limestone, 0.25%. However, the area of exposure of the igneous rocks is 25% of the total land area, while the area of the exposure of sedimentary rocks is 75%. Metamorphic rocks are formed by recrystallization under heat and pressure of the igneous and sedimentary rocks. In this discussion, these are regarded as belonging to their initial types.

Table 1 (after Clarke), shows the chemical composition of rocks. This table shows that fifteen elements constitute at least 99.75% of the earth's crust, and of these, only about nine can be regarded as at all common for any particular formation. It is seen that irrespective of the nature of the rock to be analysed, whether it be igneous or sedimentary, there is a predominance of silicon and aluminum oxides. There are also, in appreciable percentages, several other elements present (Fe, Ca, Na, K, and Mg.). It is quite an involved task to make a chemical qualitative and quantitative analysis with such a complexity of elements.

The number of elements in the sample is not the only difficulty encountered in a chemical analysis. Small samples of a few grams are used, and it is very important that homogeneity is obtained. This is usually done

by pulverizing the rock to a very fine grade, about a 200 mesh, and then by thoroughly mixing the sample. All this would be avoided in an induced radiation analysis.

In some industrial processes, such as the manufacture of manganese steel, analytical controls are essential. This makes rapid analyses necessary. Induced radiation may possibly provide a means of supplying control analyses in less time than by prevailing methods.

If analysis by using the scintillation spectrometer can remove some of the difficulties of analysis by chemical processes, then it would be a great boon to the geologist and especially to the mining industry.

TABLE 1.

| Constituent                    | A            | B             | C             | D            | E            |
|--------------------------------|--------------|---------------|---------------|--------------|--------------|
| SiO <sub>2</sub>               | 59.14        | 58.10         | 78.33         | 5.19         | 57.95        |
| Al <sub>2</sub> O <sub>3</sub> | 15.34        | 15.40         | 4.77          | 0.81         | 13.39        |
| CaO                            | 5.08         | 3.11          | 5.50          | 42.57        | 5.89         |
| Na <sub>2</sub> O              | 3.84         | 1.30          | 0.45          | 0.05         | 1.13         |
| FeO                            | 3.80         | 2.45          | 0.30          | —            | 2.08         |
| MgO                            | 3.49         | 2.44          | 1.16          | 7.89         | 2.65         |
| K <sub>2</sub> O               | 3.13         | 3.24          | 1.31          | 0.33         | 2.86         |
| Fe <sub>2</sub> O <sub>3</sub> | 3.08         | 4.02          | 1.07          | 0.54         | 3.47         |
| H <sub>2</sub> O               | 1.15         | 5.00          | 1.63          | 0.77         | 3.23         |
| TiO <sub>2</sub>               | 1.05         | 0.65          | 0.25          | 0.06         | 0.57         |
| P <sub>2</sub> O <sub>5</sub>  | 0.30         | 0.17          | 0.08          | 0.04         | 0.13         |
| CO <sub>2</sub>                | 0.10         | 2.63          | 5.03          | 41.54        | 5.38         |
| SO <sub>3</sub>                | —            | 0.64          | 0.07          | 0.05         | 0.54         |
| BaO                            | 0.06         | 0.05          | 0.05          | —            | —            |
| C                              | —            | 0.80          | —             | —            | 0.66         |
| Total                          | <u>99.56</u> | <u>100.00</u> | <u>100.00</u> | <u>99.84</u> | <u>99.93</u> |

Chemical composition of Rocks (after Clarke).

A - average igneous rocks

B - average shale

C - average sandstone

D - average limestone

E - average sediment.



## REVIEW OF LITERATURE

Nuclear Data, NBS Circular 499 of the National Bureau of Standards, is a storehouse of information of all the elements. It gives, among other things,

- (1) the percentage abundance of the elements in materials from different sources.
- (2) the slow, thermal and fast neutron cross section of all the elements.
- (3) the decay scheme and half lives of the isotopes formed from every element.
- (4) the types of reactions and the threshold energy for each reaction.
- (5) the energies of the particles given off in transitions from different energy levels.

The importance of this compilation in tagging elements by a study of the characteristics of their isotopes, can scarcely be exaggerated. If a radioelement has its half life determined, and if the gamma ray energy is known, then knowing what elements to expect in different rock formations, one can fairly well tag the element involved. Suppose for example, a sample of sand is to be studied. After irradiation with slow neutrons, it is found that the half life is 2.3 minutes, and that

the predominant line of the energy spectrum is the 1.8 mev. line. Consulting the NBS Circular would show that while  $Tl^{209}$ ,  $Ac^{223}$ ,  $Al^{28}$ , and  $Ag^{108}$  have half lives of  $2.3 \pm 0.1$  minutes, only  $Al^{28}$  has associated with it a gamma ray of 1.8 mev. A study of geology would show that aluminum and silicon are the most abundant elements in sands, and so it can be concluded that the predominant isotope is  $Al^{28}$  and thus the element involved is  $Al^{27}$ . Table 2 was culled from Nuclear Data and contains the pertinent data of the elements usually found in rocks.

G.G. Eicholz (16), of the Mines Branch, Ottawa, worked on the possibility of assaying the tantalum content in ores. A chemical analysis of this element is quite difficult, as it has a close similarity with niobium. However, tantalum<sup>182</sup>, formed by bombarding  $Ta^{181}$  with slow neutrons has a long half life (123.5 days). The associated radiation is a high energy gamma ray (0.171 mev.), and the neutron cross section is very high (21 barns). Niobium, on the other hand has a smaller cross section for thermal neutrons (1.4 barns). The isotope formed,  $Nb^{94}$ , has a comparatively short half life (6.6 minutes), and an associated gamma ray of 0.04 mev. Eicholz used a sample of about 300 - 400 mg. and three neutron sources; the Chalk River NRK pile, a 400 mg. Ra.Be source and a 500 mg. Ra.Be source. He irradiated the sample for various pre-

determined times and let the 'hot sample' cool for a day or two, during which time the isotopes of the other elements present in the sample decayed, and left only the tantalum activity.

A.M.Gaudin, F.E.Sentfle and W.L.Freyberger (2) also did some research on the induced radioactivity in natural elements. They purified their samples by picking out, by means of the Superpanner and by a special device for sorting under the microscope, those grains of elements in the ore, which seemed to have no mechanically attached impurities. Two samples were used, one for beta counting and the other for gamma counting. A small medicine capsule was used as the sample container, and a Geiger Mueller Counter was used for the detection of the gamma rays. The sample was irradiated for 2.5 sec. in the Brookhaven National Laboratory, where the neutron flux was  $10^{12} - 10^{13}$  neutrons per  $\text{cm}^2$  per sec. About 40 sec. after irradiation, counting was begun for 15 sec. intervals for a period of 5 minutes. Gaudin et al. found that it was possible to select the element in each sample which contributed the major portion of the calculated activity. It was found that there was a considerable spread of measured activities among specimens of the same mineral species, and that this reduced the resolution between mineral species, and

limited to a certain extent, the effectiveness of a separation based on the values of initial activities.

TABLE 2  
Nuclear Data for Slow Neutron Activation.

| Element | Target Nucleus    | Abundance |               | Isotopes produced | Half life        | Energy of $\gamma$ ray, mev.      |
|---------|-------------------|-----------|---------------|-------------------|------------------|-----------------------------------|
|         |                   | %         | barns         |                   |                  |                                   |
| Al.     | Al <sup>27</sup>  | 100.00    | 00.21         | Al <sup>28</sup>  | 2.3m             | 1.8                               |
| Ag.     | Ag <sup>107</sup> | 51.35     | 44.00         | Ag <sup>108</sup> | 2.33m            | ---                               |
|         | Ag <sup>109</sup> | 48.65     | 2.00<br>97.00 | Ag <sup>110</sup> | 270.00d<br>24.5s | 0.6, 0.89,<br>0.94, 1.39,<br>1.5. |
| Ca.     | Ca <sup>44</sup>  | 2.13      | 0.60          | Ca <sup>45</sup>  | 152.00d          | ---                               |
| Cu.     | Cu <sup>63</sup>  | 69.09     | 2.80          | Cu <sup>64</sup>  | 12.88h           | 1.34.                             |
|         | Cu <sup>65</sup>  | 30.91     | 1.80          | Cu <sup>66</sup>  | 4.34m            | 1.32.                             |
| Fe.     | Fe <sup>54</sup>  | 5.90      | ----          | Fe <sup>55</sup>  | 2.91y            | ----                              |
|         | Fe <sup>58</sup>  | 0.33      | 0.36          | Fe <sup>59</sup>  | 46.3d            | 1.1, 1.3.                         |
| Mg      | Mg <sup>26</sup>  | 11.00     | 0.05          | Mg <sup>27</sup>  | 9.58m            | 1.01, 0.84,                       |
| Mn      | Mn <sup>55</sup>  | 100.00    | 13.00         | Mn <sup>56</sup>  | 2.59h            | 2.13, 1.81,                       |
| Na.     | Na <sup>23</sup>  | 100.00    | 0.60          | Na <sup>24</sup>  | 14.8h            | 2.76, 1.38.                       |
| Ni.     | Ni <sup>58</sup>  | 68.00     | 4.20          | Ni <sup>59</sup>  | 1.5x10y          | ----                              |
|         | Ni <sup>62</sup>  | 3.66      | 14.80         | Ni <sup>63</sup>  | 85.00y           | ----                              |
| Si.     | Si <sup>30</sup>  | 3.12      | 0.12          | Si <sup>31</sup>  | 2.7h             | ----                              |
| Sn      | Sn <sup>112</sup> | 1.01      | 1.10          | Sn <sup>113</sup> | 113.00d          | 0.09.                             |
|         | Sn <sup>116</sup> | 14.28     | ----          | Sn <sup>117</sup> | 14.5d            | 0.175.                            |
|         | Sn <sup>122</sup> | 4.74      | 0.30          | Sn <sup>123</sup> | 41.0m            | 0.153.                            |
| V.      | V <sup>51</sup>   | 100.00    | 4.50          | V <sup>52</sup>   | 3.74d            | 1.45.                             |

TABLE 2 (Cont'd)

| Element | Target Nucleus   | Abundance % | cross section barns | Isotopes produced | Half life             | Energy of $\gamma$ ray, mev.        |
|---------|------------------|-------------|---------------------|-------------------|-----------------------|-------------------------------------|
| W.      | W <sup>180</sup> | 0.13        | ---                 | W <sup>181</sup>  | 140.0d                | 1.83                                |
|         | W <sup>184</sup> | 30.64       | 2.10                | W <sup>185</sup>  | 73.0d                 | 0.134.                              |
|         | W <sup>186</sup> | 28.64       | 34.00               | W <sup>187</sup>  | 24.1h                 | 0.48, 0.133<br>0.62, 0.68<br>0.078. |
| Zn.     | Zn <sup>64</sup> | 48.88       | 0.51                | Zn <sup>65</sup>  | 250.0d                | 1.1.                                |
|         | Zn <sup>68</sup> | 18.11       | 0.89                | Zn <sup>69</sup>  | 13.8h                 | 0.439.                              |
|         | Zn <sup>70</sup> | 0.69        | 0.085               | Zn <sup>71</sup>  | 2.2m                  | -----                               |
| Cr.     | Cr <sup>50</sup> | 4.41        | 11.00               | Cr <sup>51</sup>  | 26.5d                 | 0.32, 0.27.                         |
| K.      | K <sup>39</sup>  | 93.08       | 3.00                | K <sup>40</sup>   | 1.3x10 <sup>4</sup> y | 1.45.                               |

## DESCRIPTION OF APPARATUS

The general procedure of the experiment can be understood by an examination of the schematic diagram shown in fig.2. A large sodium iodide, thallium activated crystal, two inches in diameter and two inches high, was used throughout the experiment. This crystal was chosen because

- (1) the efficiency in converting the energy of the  $\gamma$  ray into visible radiations is very high. It is estimated that a good NaI (Tl) crystal can produce up to  $4 \times 10^4$  photoelectrons per mev. of incident radiation from the cathode of one of the latest types of photomultiplier tubes.
- (2) the light flashes produced are in the wave length band of about  $4000\text{\AA}$  in which the self absorption of the crystal is low, and at which wavelength, the cathode of the photomultiplier tube is sensitive.
- (3) the presence of iodine,  $I^{127}$ , ensures a large cross section for the photoelectric effect, especially at low energies.

formerly, the hygroscopic properties of the NaI(Tl) crystal made continuing cleaning and polishing of the crystal necessary. However, Harshaw and Co. have mounted crystals in a very thin aluminum container, with a thin disc of glass over the face of the crystal. This arrange-

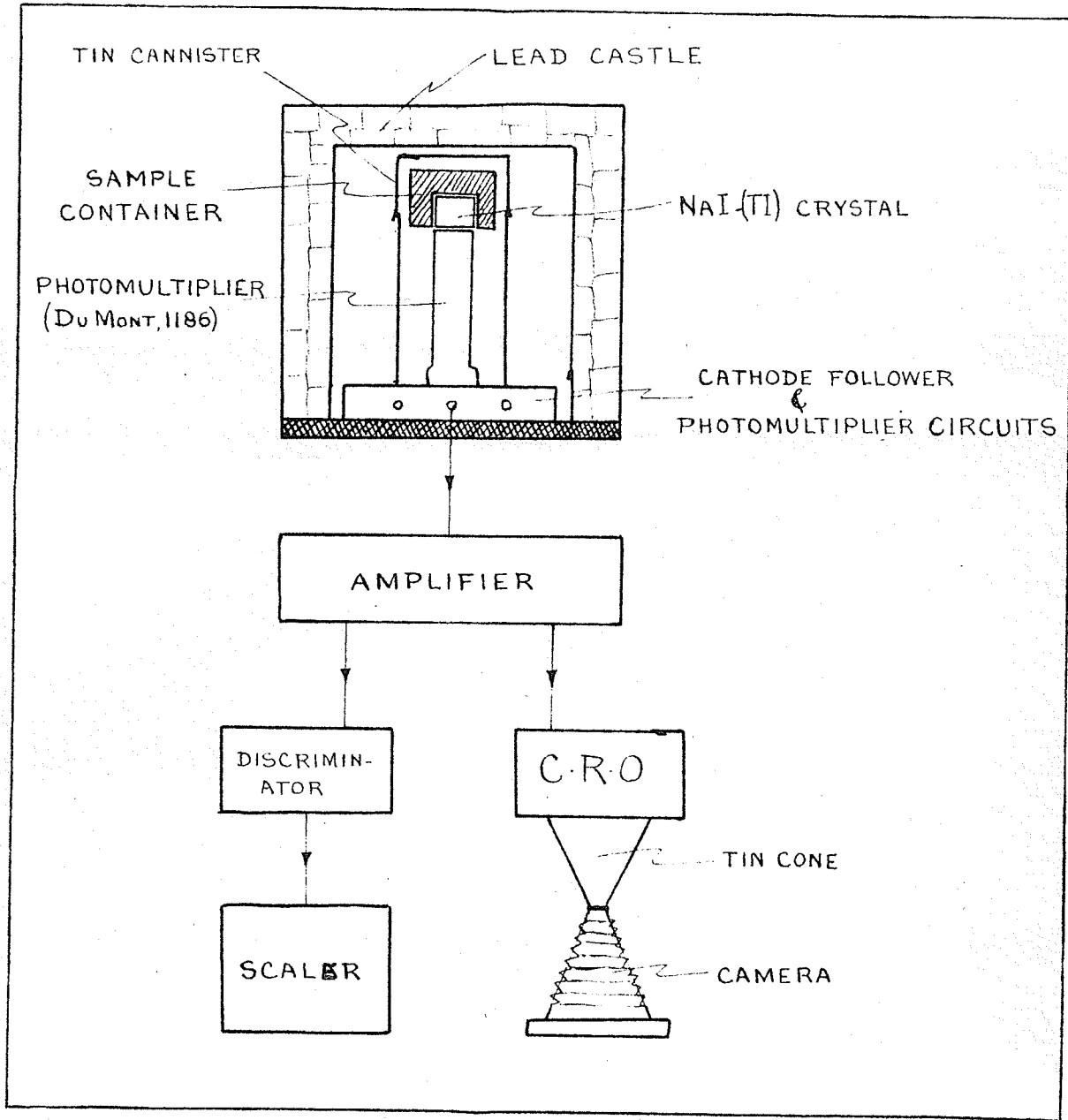


FIG. 3  
SCHEMATIC DIAGRAM OF APPARATUS.

ment keeps the crystal dry and protected against scratches. Silicone oil is used on the face of the crystal to form a tight bond between the crystal face and that of the photomultiplier.

The photomultiplier tube used is one of the latest Du Mont tubes, having a two inch photosensitive face and ten dynodes. This tube is much better than the older EMI or RCA tubes, as it has a uniform photosensitive surface of high efficiency, and a high amplification factor. Ten megohm resistances were soldered between adjacent dynodes and between the first and second dynodes, a 20 megohm resistor was used. This produced a larger voltage drop between the first two dynodes, and this was found to produce a slightly higher resolution. The tube is rated as having a gain of about  $10^6$  for 100 volts per dynode and a higher gain at 150 volts per stage.

The circuit of the laboratory-made amplifier is shown in fig. 3. This is basically the same design as the last stage of the Atomic Instrument Co's Model 204C amplifier. The amplification is in four stages, the total gain being about 60.

The discriminator was built in this laboratory. The circuit diagram is shown in fig. 4. It was designed by



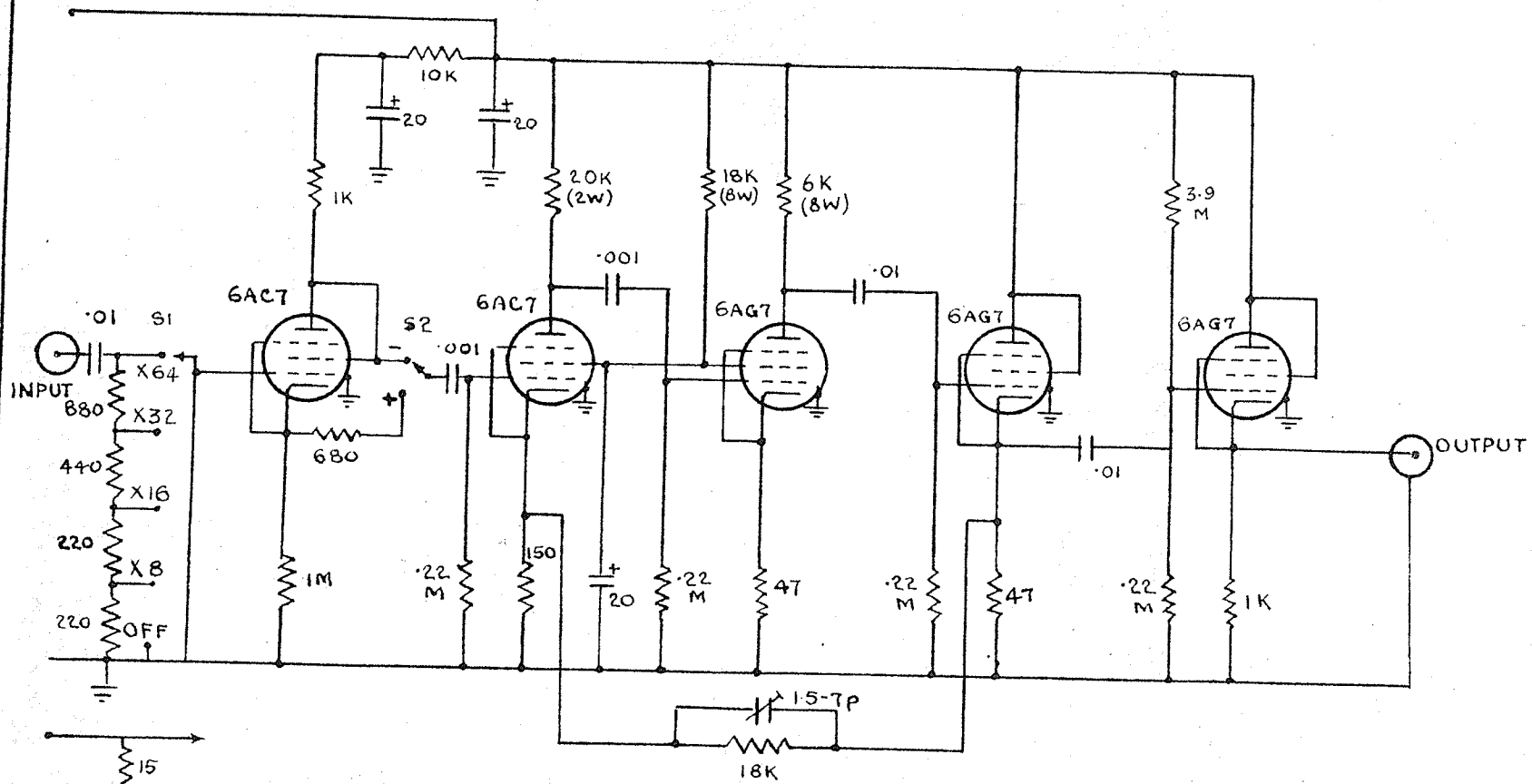
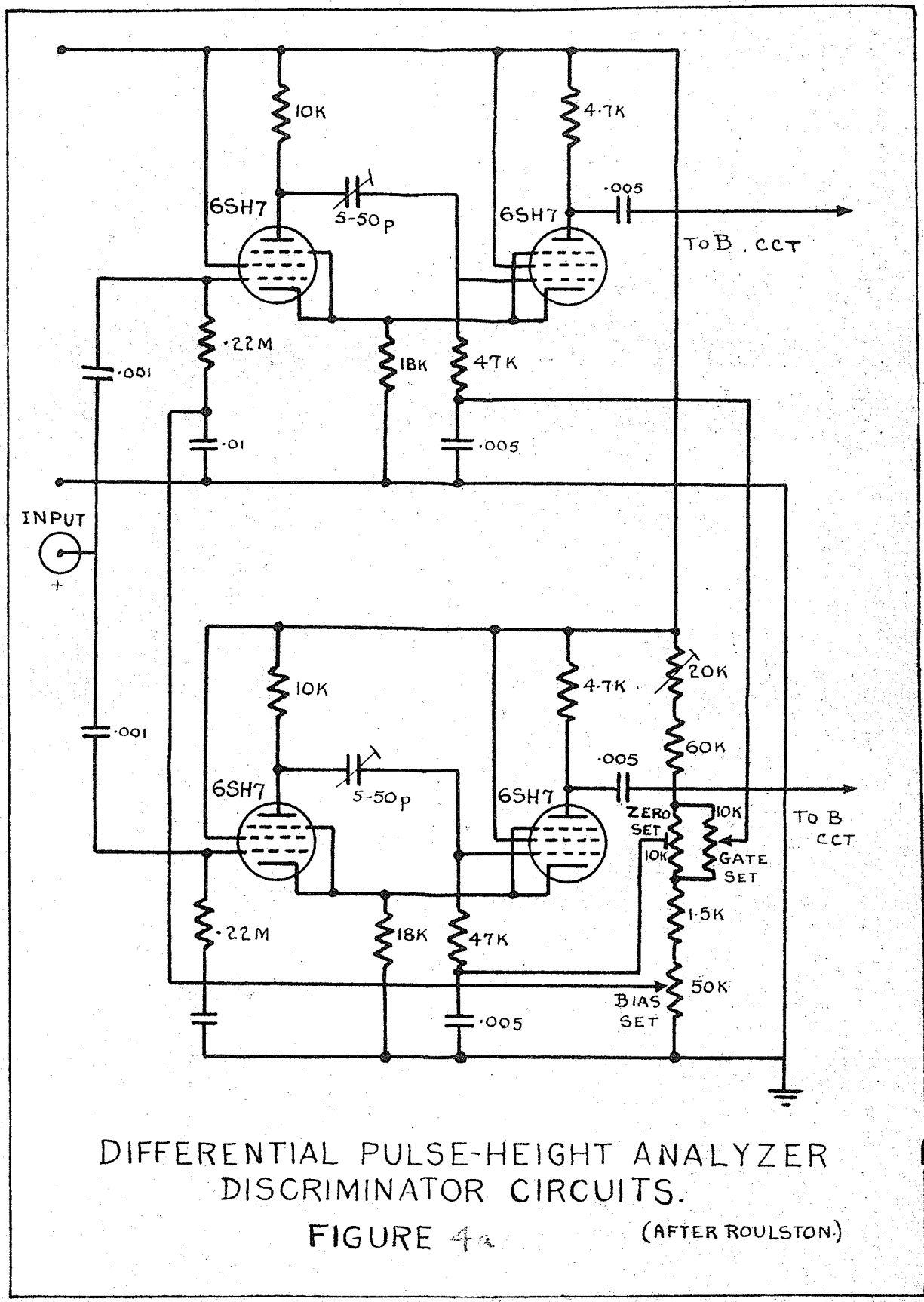


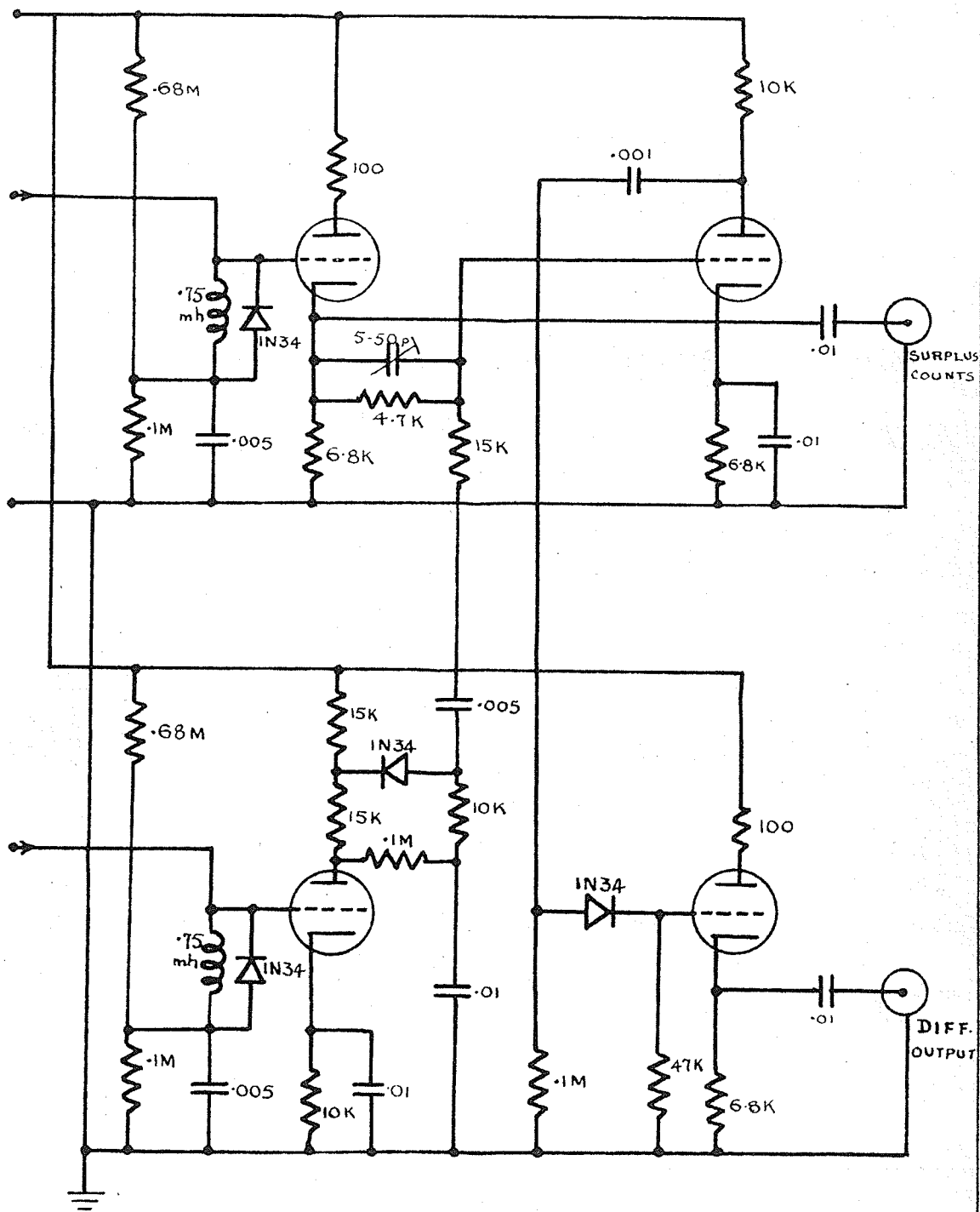
FIG. 5.  
 LINEAR AMPLIFIER



DIFFERENTIAL PULSE-HEIGHT ANALYZER  
DISCRIMINATOR CIRCUITS.

FIGURE 4a

(AFTER ROULSTON)



DIFFERENTIAL PULSE-HEIGHT ANALYZER  
 (B) ANTI-COINCIDENCE CIRCUIT.

FIGURE 4b (AFTER ROULSTON)

Dr. K.I. Roulston (17) of the University of Manitoba. It is seen that the circuit consists of two modified Schmitt trigger circuits. When one bank is used, the discriminator is used as an integral discriminator, and by using both banks, it is used as a differential discriminator.

The first tube of each bank is biased beyond cutoff, and a positive pulse exceeding this biasing voltage triggers the circuit. This pulse is taken off the plate of the first tube through a coupling condenser to the second tube. This makes the cathode potential smaller, and thus the current in the first tube is increased. The process is cumulative, and the second tube is soon cut off. The positive pulse which appears on the plate of the second tube is of constant amplitude. This pulse is applied to an inductance and a crystal diode in parallel, and the output is a half sine wave whose duration is about 0.5 microseconds. The pulse then goes to a phase inverter. This is a double triode 6SN7. In one bank the pulse is taken off the cathode and is thus negative, and in the other, it is taken off the plate through a resistance chain, and is thus positive. If the pulses are identically the same and occur at the same time, these pulses cancel each other. However, the two discriminators do not trigger at exactly the same instant. If one tube in one

bank is biased above the corresponding tube in the other bank, then in the cancellation process, only those pulses will be obtained which correspond to the difference in the biasing voltages or the gate width. In this way, it is possible to analyse the entire spectrum or to discriminate between pulses of various voltages or energies.

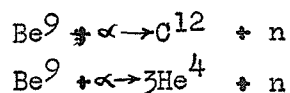
Those pulses which are larger than the bias voltage, and which pass through the discriminator, are registered on a counter. A Glow Transfer Counter, Model 162, built by the Atomic Instrument Co. in Cambridge, Mass. was used. This counter has a counting rate of zero to over 2,000 cps, and has a total counting capacity of  $10^6$  counts.

Another method used to detect the voltage pulses is to pass the pulses from the amplifier to a cathode ray oscilloscope, and have them displayed on the screen. A Tektronix model 511AD C.R.O. is used, and in order to record the waveforms, photographs are taken with an f=4.5 lens camera.

Two regulated power supplies, manufactured by the Lambda Electronic Corporation, Corona, New York, Model No.28, are used to supply filament and plate voltages to the tubes. These power supplies have a continuously

variable dc. output from 200 to 325 volts, regulated from 0 to 100 ma. maximum. The output is rated to be constant to better than 1% for loads from zero to full load, and with line voltage variations from 105 to 125 volts. The 110 line voltage is first passed through a constant voltage transformer. The high voltage for the photomultiplier is obtained from 4 or 5, 300 volts Eveready batteries connected in series.

From an examination of Eq.5, it is seen that the amount of induced activity is directly proportional to the neutron flux and to the amount of sample used. Two Po-Be sources were used in the course of the experiment. The first was a 5 curie source, and the other about half as strong. The neutron flux of a curie of Po. is  $2.5 \times 10^6$  neutrons per sec. per  $\text{cm}^2$ . The neutrons from the Po-Be source are formed in the reactions



These neutrons are not monoenergetic because (18),

- (1) the  $\alpha$  particles of the polonium do not all have the same initial energy.
- (2) the  $\alpha$  particles lose part of their energy by collisions before they interact with a beryllium nucleus.
- (3) the  $\text{C}^{12}$  formed, may be in an excited state.
- (4) there are two different reactions.

It was necessary for the safety of the personnel, and for keeping the background counting rate as low as possible to house these sources properly. Fig.5 shows the housing used. It consists of a large cylindrical tank,  $4\frac{1}{2}$  feet in diameter by 3 feet high, and an inner tank, 2 feet in diameter by  $2\frac{1}{2}$  feet high. The inner tank was off-centred to provide greater shielding on one side of the tank. A chlorine-free plastic cylinder, which was sealed at one end, and which was 18 inches long and 4 inches in diameter was inserted in the centre of the inner tank. Ten inches of the tube was in the oil. The neutron source was placed in the bottom of the tube, and 5.75 cm. of paraffin put on the source. This amount of paraffin was found sufficient to thermalize the fast neutrons. Since hydrogenous matter thermalizes fast neutrons, the outer tank was filled with water, and the inner tank was filled with transformer oil. To provide additional shielding and protection, boron in the form of borax was dissolved in the water. The efficiency of the tank design was tested by measuring the activity at various points around and away from the tank with a portable scintillometer. At point A, shown in Fig 5(a), the rete meter showed a deflection of 1450, and at the nearest point to the crystal, point B, the deflection was 970. The design was therefore shown to be quite effective in providing good shielding and protection.



fig. 5a.  
Showing Neutron Source Housing



fig. 5b.  
Showing Sample Containers



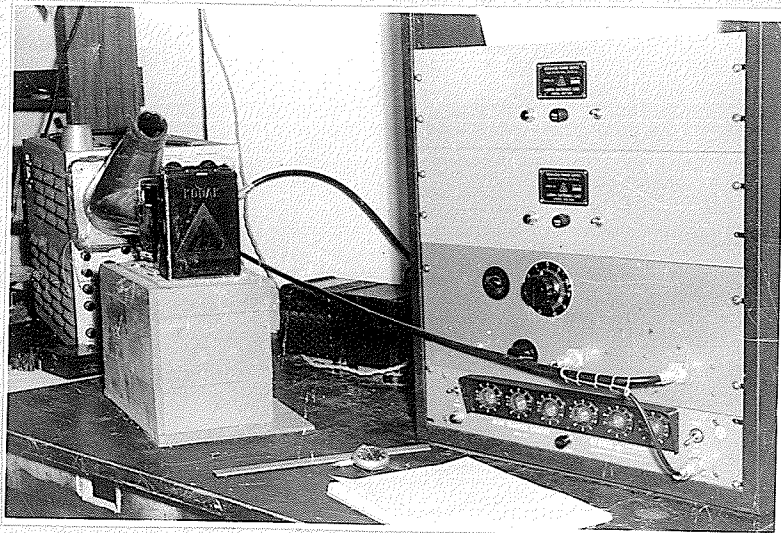


fig. 5c.  
Showing layout of Apparatus



fig. 5d.  
Showing Photomultiplier Tube Housing  
and Cathode Follower in Lead Castle

(3)

The material to be studied is put in the sample container shown in fig. 5 (b). This is also built of plastic free from chlorine. This was necessary since chlorine,  $Cl^{35}$ , has an appreciable cross section for thermal neutrons. The container was shaped so that the best geometry is obtained. It is seen that almost the entire crystal is enveloped.

## PRELIMINARY INVESTIGATIONS.

Before the neutron-capture experiment on any element was done, it was necessary to carry out some preliminary investigations.

First, the discriminator had to be calibrated. This was done by plotting a differential curve of the  $\text{Cs}^{137}$  spectrum. The graph obtained is shown in fig.6. It is seen that the 665 kev. energy peak occurs at a dial setting of 5.5. From this relationship, the settings on the dial of the discriminator was calibrated in terms of gamma ray energy. To minimize the background counting rate, the dial was set so that only pulses greater than 100 kev. were counted.

It was also necessary to determine the amount and structure of the sample to be used. The activation of an element has been shown to be proportional to the mass of the element in the sample, and since the background from the neutron sources was quite high, ( $\approx 1000$  cpm), a sufficiently large sample had to be used so that the counts upon activation were higher than the background counts. This minimized errors due to statistical fluctuations. Since the sample is not 'destroyed' as is done in a chemical analysis it was also practical to use a large sample. A sample of 400 grams was found most convenient. Also, in a chemical

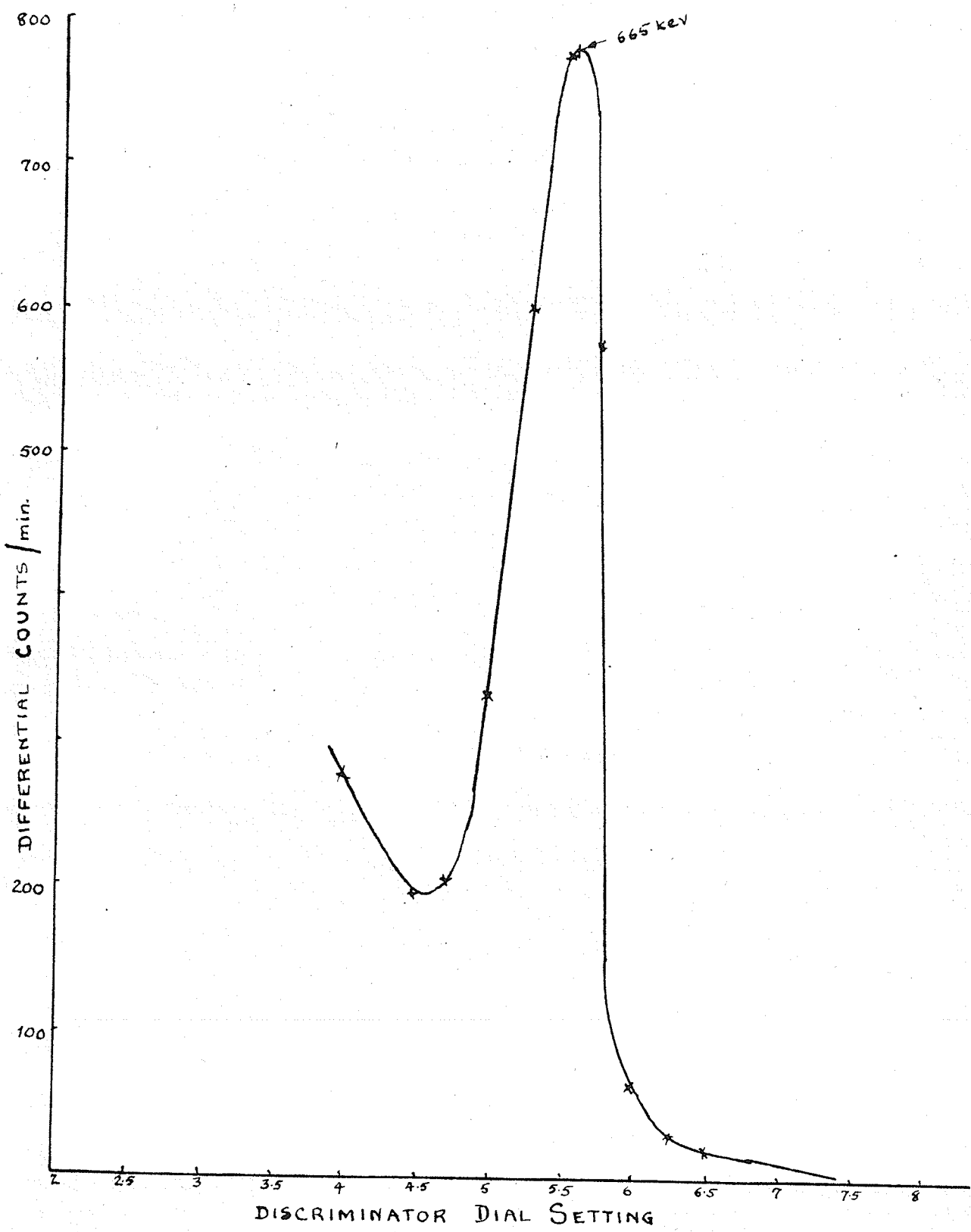


FIG. 6.  
SPECTRUM OF  $Cs^{137}$

analysis, the sample is usually crushed to a powder. Various grain sizes of samples were tested, and it was found that pulverizing to a powder was not necessary. The only requirement, in regard to the structure of the sample is that it be broken into pieces about  $\frac{1}{4}$ " in diameter.

In industry, time is a very important factor in rock analysis. The irradiation period of the sample should be the shortest irradiation time required to produce an induced counting rate sufficiently above background (about 2 or 3 times background). Experiments were performed on samples using different irradiation periods, and it was found that a 4.5 minute irradiation for most samples gave a counting rate which was much higher than background.

Certain corrections were made on the results obtained.

- (1) Comparison of the initial counting rates could easily be made if the amount of sample used in all the experiments were of a standard amount. The activation of the samples which were smaller, had to be corrected by simple proportion to give the activity of a sample of the standard weight.
- (2) The background, that is the pre-activation counts of the sample and container, which was due to the presence of stray neutrons, traces of radioactive elements in the sample to be studied, and cosmic rays, was

subtracted from the total number of counts obtained after irradiation. In this manner the actual number of counts from the sample were obtained. The container was placed over the neutron source for half an hour, but it gave no activation counts.

- (3) The neutron sources used in these studies have a definite period of decay. This is due to the decay of polonium,  $\text{Po}^{210}$ , which has a half life of 138.9 days. The actual neutron flux thus changes daily. Since the number of counts after activation is directly proportional to the neutron flux, correction had to be made for this changing flux.
- (4) There was a 30 sec. time lag due to the transfer of the sample between the end of the activation period and the beginning of the counting period. The graphs, showing the decay of the isotopes formed during and after the irradiation period, and which were plotted on semi-log graph paper, were extrapolated to include this time lag, and the number of counts at time,  $t = 0$ , were obtained.

All the activation numbers given in the report are the corrected values, and shall be designated henceforth as 'initial' counts.

## ACTIVATION ANALYSIS OF CERTAIN ELEMENTS

In the following pages, the experiments performed on the elements commonly found in rocks will be discussed. These elements include aluminum, silicon, silver, manganese, copper, and magnesium. Experiments performed to determine the difference in activation counting rate of shales, sandstones and limestones, will then follow.

The first element to be experimented on was aluminum.

## ALUMINUM

In the outer part of the earth's crust, aluminum is the most abundant metal. Because of its strength and lightness it is becoming increasingly popular in industry. It is used chiefly in alloys, and a fast determination of the percentage of aluminum in alloys would be very useful. The following experiments on aluminum were preliminary investigations with this thought in view.

From table 1 it is seen that aluminum occurs always as  $\text{Al}^{27}$ . Its cross section for thermal neutrons is 0.21 barns, and upon activation, the isotope  $\text{Al}^{28}$  is formed.  $\text{Al}^{28}$  has a half life of 2.3 minutes, and decays by  $\beta^-$  emission of 3.01 mev. and then by  $\gamma$  emission of 1.8 mev. to stable  $\text{Si}^{28}$ . This isotope ( $\text{Si}^{28}$ ) has no reported cross section for thermal neutrons.

An aluminum casting which weighed 320 grams, and so shaped as to fit snugly over the crystal, was tested. The casting was placed on the blocks of paraffin (5.75 cm) which thermalized the neutrons, and it was irradiated for 4.5 min. After the activation period, the 'hot' sample was placed on the crystal, and after the 30 second lag allowed for transferring the sample to the spectrometer, an integral counting rate determination was begun. The

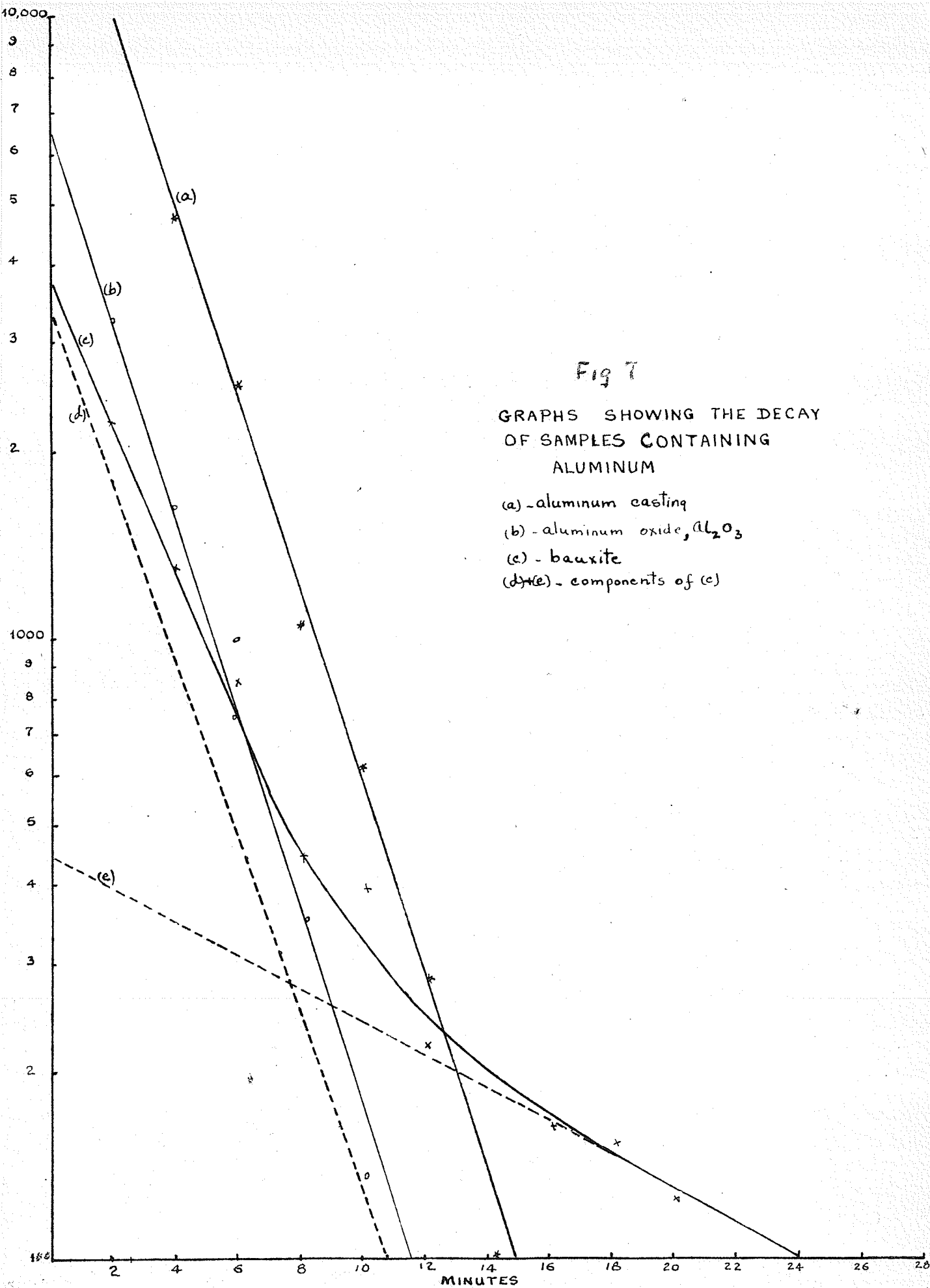


number of counts were plotted against time, on semi-log graph paper, and the curve obtained is shown in fig.7a. A photograph of the spectrum was taken at an exposure time of 10 minutes. This is shown in fig. 8.

The same experimental procedure used in the activation of the aluminum casting, was followed for samples of 200 grams of  $Al_2O_3$ , and 200 grams of bauxite. The  $Al_2O_3$  sample contains 108 grams of aluminum, and its decay curve is shown in fig. 7b. The bauxite was assayed by the Mines Branch in Winnipeg, at 55.47%  $Al_2O_3$ . The sample therefore contained 48 grams  $Al^{27}$ . The decay curve obtained after activation is shown in fig. 7c, and the photograph of the decaying isotopes is shown in fig.9.

#### DISCUSSION

The half life of the isotope produced by the activation of the aluminum casting, and calculated from the decay curve shown in fig.7a, is 2.1 minutes. The same half life value is obtained from the sample of  $Al_2O_3$ . This agrees with the recorded value of 2.3 minutes for  $Al^{28}$ . After the necessary corrections had been made, and by extrapolation to  $t = 0$ , the 'initial' activation counts were



found to be 23,000 counts per two minutes, and 7,650 counts per two min. for the aluminum casting and the sample of  $Al_2O_3$  respectively. This gives an activation per gram of 72 and 71 counts per 2 minutes.

The decay curve for the bauxite sample, fig.7c, is different in shape. It is observed that the decay is not that of the  $Al^{28}$  only. This curve was resolved into its component parts and the half lives of the two elements indicated were 2.2 min. and 11 min. The 2.2 min. half life is undoubtedly the  $Al^{28}$  half life. The longer half life component could be that of  $Al^{29}$ , which has a half life of 7 minutes, and which is formed by a  $Si^{29} (n,p)Al^{29}$  reaction. It is to be remembered that  $Si^{29}$  would be present in the bauxite sample as an impurity, and that if all the neutrons were not thermalized, the (n,p) reaction on the  $Si^{29}$  (4.7% abundance and a cross section of 2.7mb. for energies of about 1 mev.), is possible. This would account for the longer lived half life (11 min.) as shown on the graph in fig.7e.

The photograph shown in fig.9 shows that the spectrum of the activated bauxite is blocked. However, the trailing edge of the  $1.8Al^{28}$  energy line is quite distinct. The  $Cs^{137}$  (0.665 mev.) calibration spectrum is shown on the right of

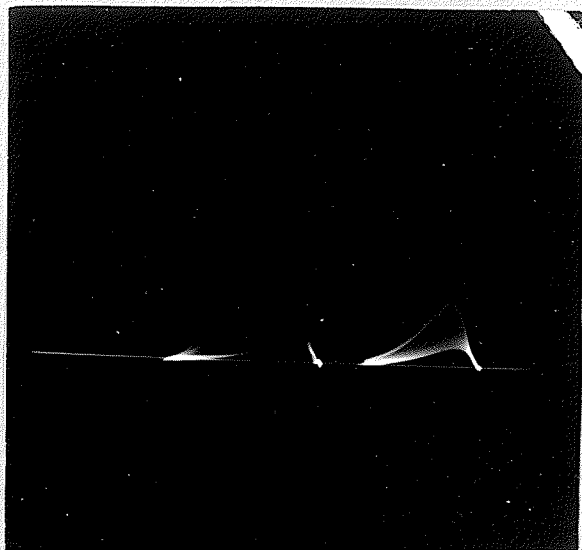


fig. 8.

Spectrum of Activated Aluminum Casting

Spectrum of Cs<sup>137</sup> on right



fig. 9.

Spectrum of Activated Bauxite

Spectrum of Cs<sup>137</sup> on left.

the photograph. The line corresponding to the energy of the longer half life component as shown on the decay curve is not observed in this picture. This might be due to the film exposure time not being long enough, or to the intensity of the gamma ray not being strong enough.

The photograph of the spectrum of the activated aluminum casting, shown in fig. 8, with 1200 volts on the photomultiplier tube to prevent blocking, shows the 1.8 mev. energy line of  $\text{Al}^{28}$ . The  $\text{Cs}^{137}$  calibration line is shown on the left. The difference in the intensities of the spectra shown in fig. 8 and fig. 9 is due mainly to the difference in the voltages applied to the photomultiplier tube.

#### CONCLUSION

Considering the aluminum casting as the standard sample, the number of counts per gram per 2 minutes of aluminum is 72. The 'initial' number of counts per 2 min. corrected for a time lag of 30 sec. is 7,650 for the activated  $\text{Al}_2\text{O}_3$ . By simple proportion, this corresponds to an aluminum content of 106 grams. This agrees with the actual aluminum content of 108 grams, the error being 0.01. By a similar consideration, the bauxite sample which gave a corrected 'initial' number of counts per 2 min. of 3600 after activation, contains 50 grams of aluminum. This agrees



very well with the amount of aluminum (48 gm.) found by chemical assay.

These results suggest that it is possible to determine the percentage of aluminum content at least to a degree where it is considered commercially valuable.

## SILICON

An examination of table 1 shows that the silica content in all types of rocks, except limestone, is very high. The value varies from 58% in the case of sediments, to 80% for sandstones. Silicon would therefore be present in nearly all the samples to be studied, and it seemed pertinent to obtain some experimental data on its characteristics after irradiation.

In Nuclear Data, NBS Circular 499, it is noted that silicon occurs naturally as  $\text{Si}^{28}$  (92.19%),  $\text{Si}^{29}$  (4.7%) and as  $\text{Si}^{30}$  (3.12%). Of these only  $\text{Si}^{30}$  has a cross section for thermal neutrons, its value being 0.12 barns. Upon activation with thermal neutrons,  $\text{Si}^{31}$  is formed. This isotope has a half life of 2.62 hours. Nuclear Circular 499 reports no  $\gamma$  rays associated with  $\text{Si}^{31}$ . However, P.G. Cobb reported in the Purdue University Progress Report 11 (June, 1952), the existence of  $\gamma$  transitions of energy 0.17, 0.52 mev. and a questionable weak radiation of about 1 mev.

A sample of Black Island silica sand was obtained from the Mines Branch, Winnipeg. The assay on this sand was:

|                 |                               |        |
|-----------------|-------------------------------|--------|
| Silica.....     | $\text{SiO}_2$ .....          | 99.33% |
| Iron Oxide..... | $\text{Fe}_2\text{O}_3$ ..... | 0.03%  |
| Alumina.....    | $\text{Al}_2\text{O}_3$ ..... | 0.28%  |
| Lime.....       |                               | 0.12%  |

Magnesia.....0.15%

Traces of soda, potash and  
loss on ignition.....0.09%

A sample of 400 grams of this sand was irradiated for 4.5 minutes. After the necessary corrections were made on the number of counts obtained, the graph shown in fig. 10 was drawn. A photograph of the spectrum, displayed on the oscilloscope, was also taken.

#### DISCUSSION

Both the graph obtained by plotting the activation counts of the decaying isotopes and shown in fig. 10, and the photograph of the spectrum are interesting. The 'initial' activity, as found from the graph is 2750 counts per 2 minutes, and the half life obtained is 2.5 min. From the negative of the photograph could be seen the very faint trace of a line, which by calibration with the  $Cs^{137}$  line corresponded to an energy of 1.8 mev. This line could not be made darker by a longer exposure because of the short half life of the isotope present, and it could not be resolved in a print of the negative. The high number of 'initial counts' is not consistent with the low cross section, and the small amount of  $Si^{30}$  (5.5 gm.) in the sample. Also, the half life and the energy of the  $\gamma$  ray do not agree with the reported values. In fact, the characterist-



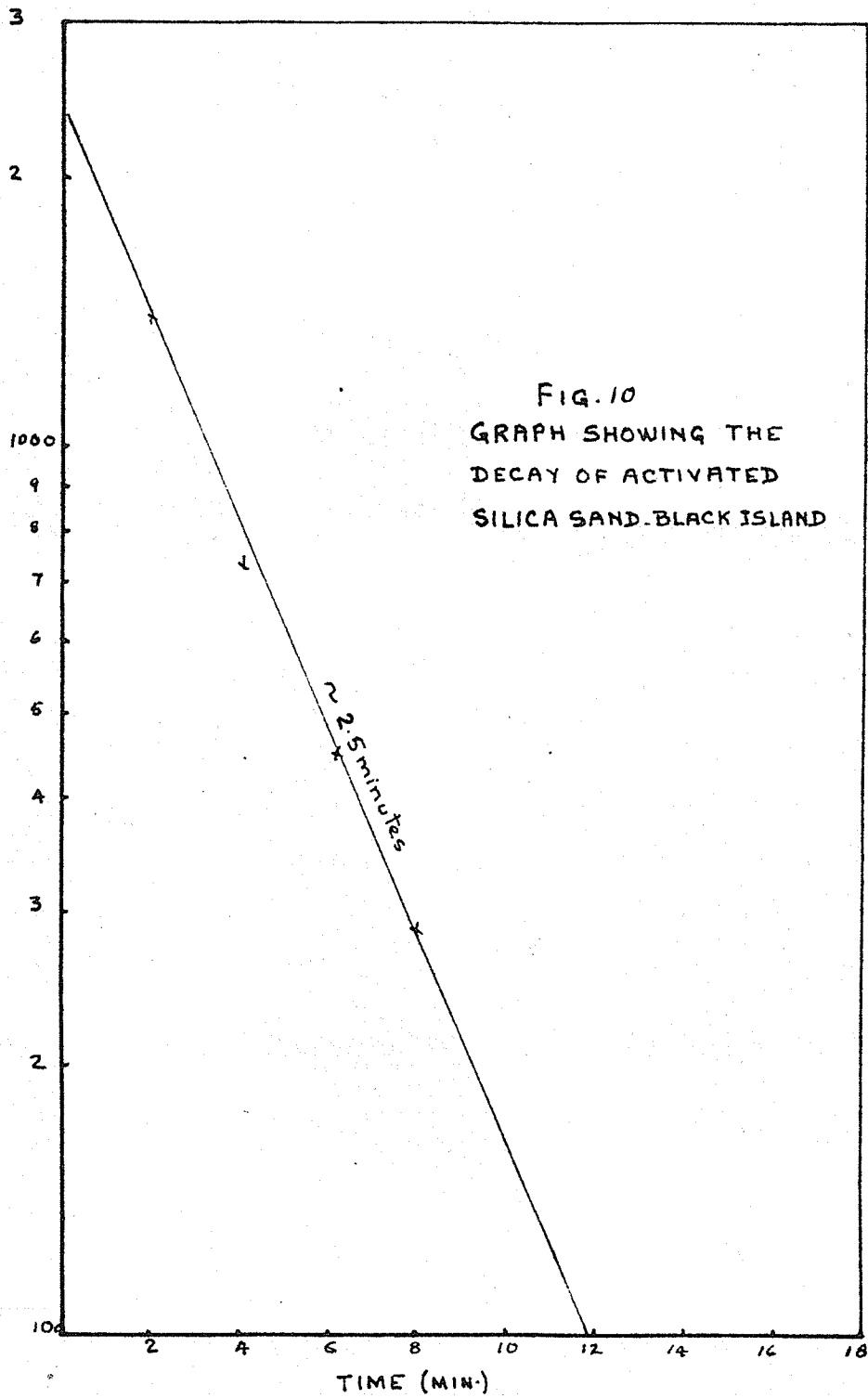


FIG. 10  
 GRAPH SHOWING THE  
 DECAY OF ACTIVATED  
 SILICA SAND. BLACK ISLAND

ics of half life (2.5 min.) and  $\gamma$  ray energy indicates very strongly the presence of  $Al^{28}$ .

The high number of 'initial' counts could be partially due to the activation of trace elements present in the sample. These included Ca, Fe, Mg, soda and potash. From the assay values, it is seen that the sand contains 0.28% alumina. A sample of 400 grams would contain 0.6 grams aluminum and 185 grams of  $Si^{28}$ . The presence of this aluminum, and the probability that all the neutrons were not thermalized and therefore the reaction  $Si^{28} (n,p) Al^{28}$  2.3 min. might have taken place, would also account for the high counting rate and the 1.8 mev. energy line.

## ALUMINUM AND SILICON

From table 1 it is seen that aluminum and silicon together constitutes more than 70% of nearly all rocks except limestone formations. From the experiments performed on aluminum, it is seen that bauxite deposits can be analysed. However, some difficulty might be encountered in analysing rocks with a lower aluminum content and a high silica content, so further experimentation was necessary. Besides being a continuation of the last experiment on the activation of silicon, it is an attempt to find out what happens to aluminum and silicon samples when they are irradiated by neutrons of different energies. It was hoped that this would lead to a method of differentiation between the two elements.

From Nuclear Data Circular 499, the reactions for  $Al^{27}$ , and  $Si^{28}$ ,  $Si^{29}$  and  $Si^{30}$  are:  
 $Al^{27}$ , abundance 100%.

| Reactions.  | Cross Section (barns) |
|---|-----------------------|
| $Al^{27}$ (th n, $\gamma$ ) 2.3 min. $Al^{28}$      | 0.21                  |
| $Al^{27}$ ( 1 mev.n, $\gamma$ )( 2.3 min. $Al^{28}$ | 0.40mb.               |
| Al ( 1 mev.n,p ) 9.6 min. $Mg^{27}$                 | 2.80mb.               |
| $Al^{27}$ ( 1 mev.n, $\alpha$ ) 14.9 hr. $Na^{24}$  | 0.60mb.               |

2.3 min.  $Al^{28}$  has one  $\gamma$  ray associated with it with an energy of 1.8 mev.

9.6 min.  $Mg^{27}$  has three  $\gamma$  rays associated with it with

energies of 1.01, 0.84 and 0.64 mev.

14.9 hr.  $\text{Na}^{24}$  has two  $\gamma$  rays associated with it with energies of 2.76 and 1.38 mev.

$\text{Si}^{28}$ , abundance 92.2%

| Reactions   | Cross Section |
|---|---------------|
| $\text{Si}^{28}$ ( $\sim$ 1mev.n,p) 2.3 min. $\text{Al}^{28}$ | 3.0mb.        |

$\text{Si}^{29}$ , abundance 4.7%

Reaction

|   |        |
|---|--------|
| $\text{Si}^{29}$ ( $\sim$ 1mev.n,p) 6.7 min. $\text{Al}^{29}$ | 2.7mb. |
|---|--------|

$\text{Si}^{30}$ , abundance 3.1%

Reaction

|   |         |
|---|---------|
| $\text{Si}^{30}$ (th n, $\gamma$ ) 2.7 hr. $\text{Si}^{31}$ | 0.12mb. |
|---|---------|

|   |         |
|---|---------|
| $\text{Si}^{30}$ ( $\sim$ 1 mev.n $\gamma$ ) 2.7 hr. $\text{Si}^{31}$ | 1.1 mb. |
|---|---------|

$\text{Al}^{28}$  has one  $\gamma$  ray associated with it with an energy of 1.8 mev.

$\text{Al}^{29}$  has two  $\gamma$  rays associated with it with energies of 2.3 and 1.2 mev.

$\text{Si}^{31}$  according to Nuclear Data, has no gamma ray.

$\text{Si}^{31}$  according to P.G. Cobb, Purdue Univ. Progress Report 11, June 1952, has three  $\gamma$  rays associated with it, with energies of 0.17, 0.52 and + 1 mev.

The aluminum sample used in this experiment was the aluminum casting used in previous experiments. This weighed 320 grams. An equal weight of silica sand was used. It is to be noted that the aluminum casting, which fitted the crystal snugly to give the best results as far as geometry is

concerned, was of the same shape as the container for the sand sample. In this way, the geometry of both samples under study was made equal.

The varying energy of the neutron flux was obtained by placing measured amounts of paraffin wax on the source. The procedure followed in the experiment was to place a known amount of paraffin on the source, and then to activate the aluminum casting. After a 4.5 minute irradiation period, the activated sample was taken to the spectrometer, and the number of counts per minute was taken. This number was then corrected for background and time lag as mentioned on page 33, and the number of 'initial' activation counts per minute obtained. The same procedure was followed for the silica sand sample, and similar readings obtained. The number of counts for each sample was plotted against the number of centimeters of paraffin on the source, and the results obtained are shown in fig. 11. Also the ratio of the initial activity of the activated aluminum sample to the initial activity of the activated silica sand sample was plotted against the number of centimeters paraffin. The results obtained are shown in fig. 12.

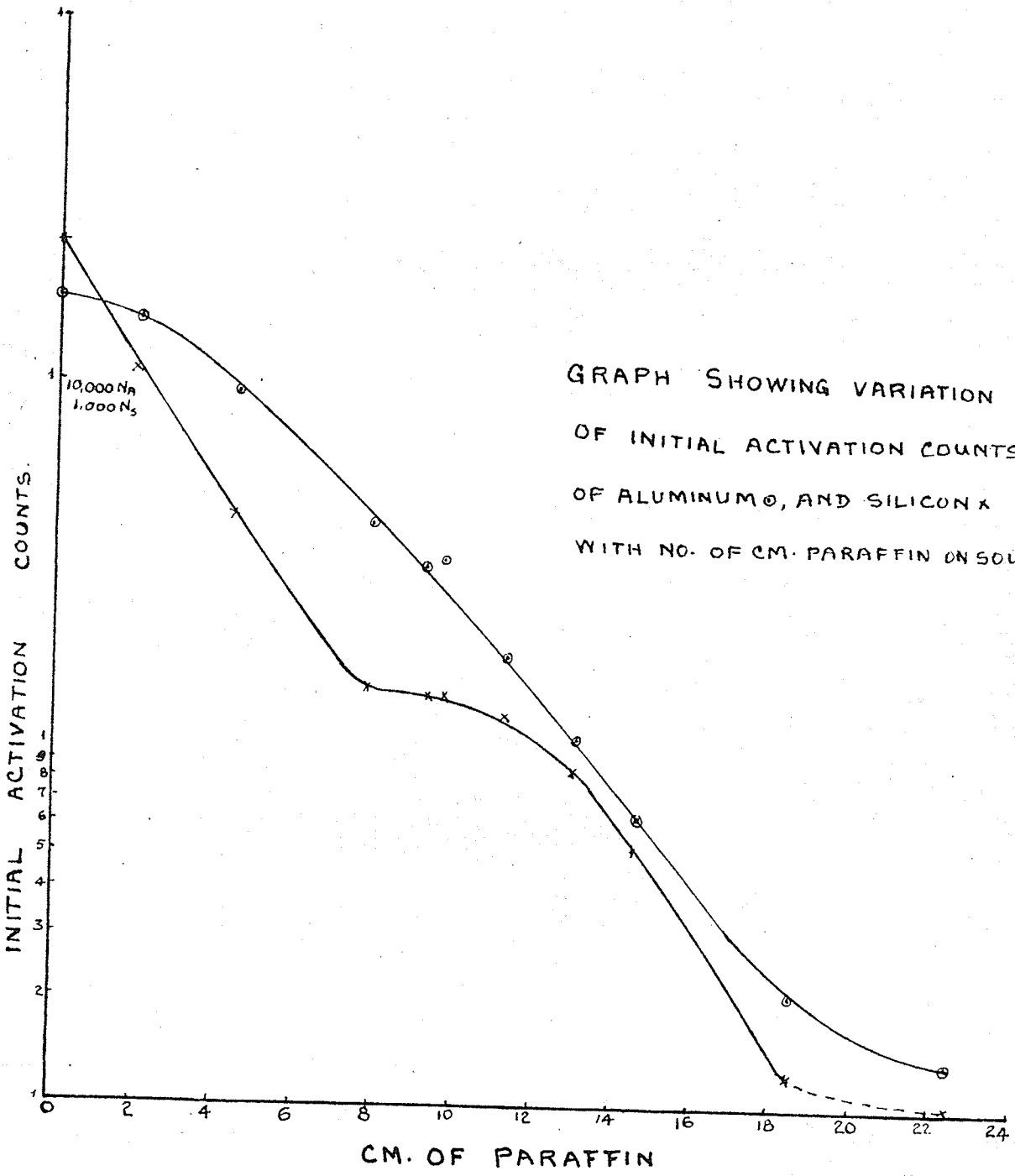


Fig. 11

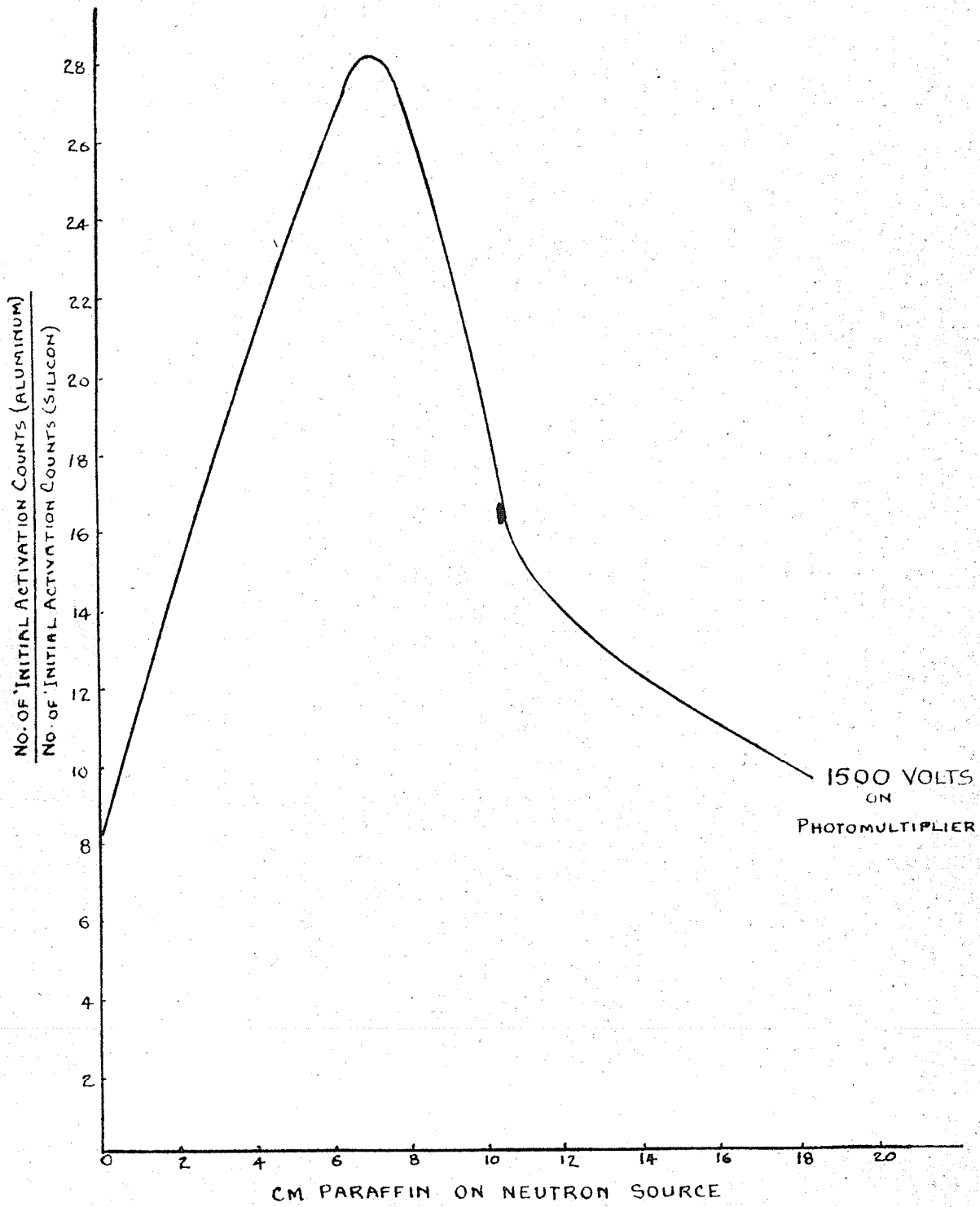


FIG. 12.

## DISCUSSION

An examination of the graphs shown in fig. 11 and 12 shows that the ratio of the activation counts of aluminum to those of silicon for neutrons of high energy is smaller than the ratio obtained for those at thermal energies. It is seen that when there is no paraffin on the source, and thus when the sample is activated by a wide range of neutrons from 2 mev. to 10 mev., the ratio of the number of counts is  $\sim 7$ . This ratio becomes linearly higher as the neutrons are thermalized, until a peak is reached. This occurs when there are about 5.75 cm. of paraffin on the source and all thermalized. The ratio is about 27. As more paraffin is placed on the source, some of the neutrons are absorbed, and the ratio of initial counts gets smaller. The decrease is almost exponential, the point of inflection occurring when there are about 11 cm. of wax on the neutron source. Examination of the graph on fig. 11 shows a hump on the curve when 8 to 10 cm. of paraffin is used. This might be the effect of resonant neutrons. There is no recorded resonant neutron effect at this low energy range, and it would be interesting to carry out more conclusive tests. However, this is of purely academic interest and not within the scope of this report.

This experiment indicates that in a sample containing



large percentages of alumina and silica, the greatest difference between the activation counts of the isotopes produced upon irradiation would be obtained by placing about 5.75 cm. of paraffin on the source.

## SILVER

Gold and silver are commonly found in the same deposit. However, there exists a few important deposits of silver that are essentially free from gold. Silver also commonly occurs with copper, lead and zinc.

In its natural state, silver occurs as  $\text{Ag}^{107}$  (51.35%) and as  $\text{Ag}^{109}$  (48.65%).  $\text{Ag}^{107}$  has a high cross section for thermal neutrons, the value being 44 barns. Upon irradiation,  $\text{Ag}^{108}$  is produced, and this isotope has a half life of 2.33 minutes. The decay to cadmium,  $\text{Cd}^{108}$ , is by a  $\beta^-$  emission, and there are no reported  $\gamma$  rays emitted.

There are two recorded cross sections for thermal neutrons on  $\text{Ag}^{109}$ , the other form of natural silver. They are 97 and 2 barns. The reactions are:

$\text{Ag}^{109}$  (th n,  $\delta$ ) 24.5 sec.  $\text{Ag}^{110}$  .....97 barns  
 $\text{Ag}^{109}$  (th n,  $\delta$ ) 270 days  $\text{Ag}^{110}$  .....2 barns

The decay scheme of  $\text{Ag}^{110}$  is quite complex, and is shown in fig. 13 (14).

Three samples of silver concentrates, designated as E27-1, E27-2 and E27-3 were obtained from Packing Ore, Silver Islet. Samples of 300 grams of each silver concentrate were irradiated for 2.5 minutes, and after activation, the counting rates per minute were recorded. The decay

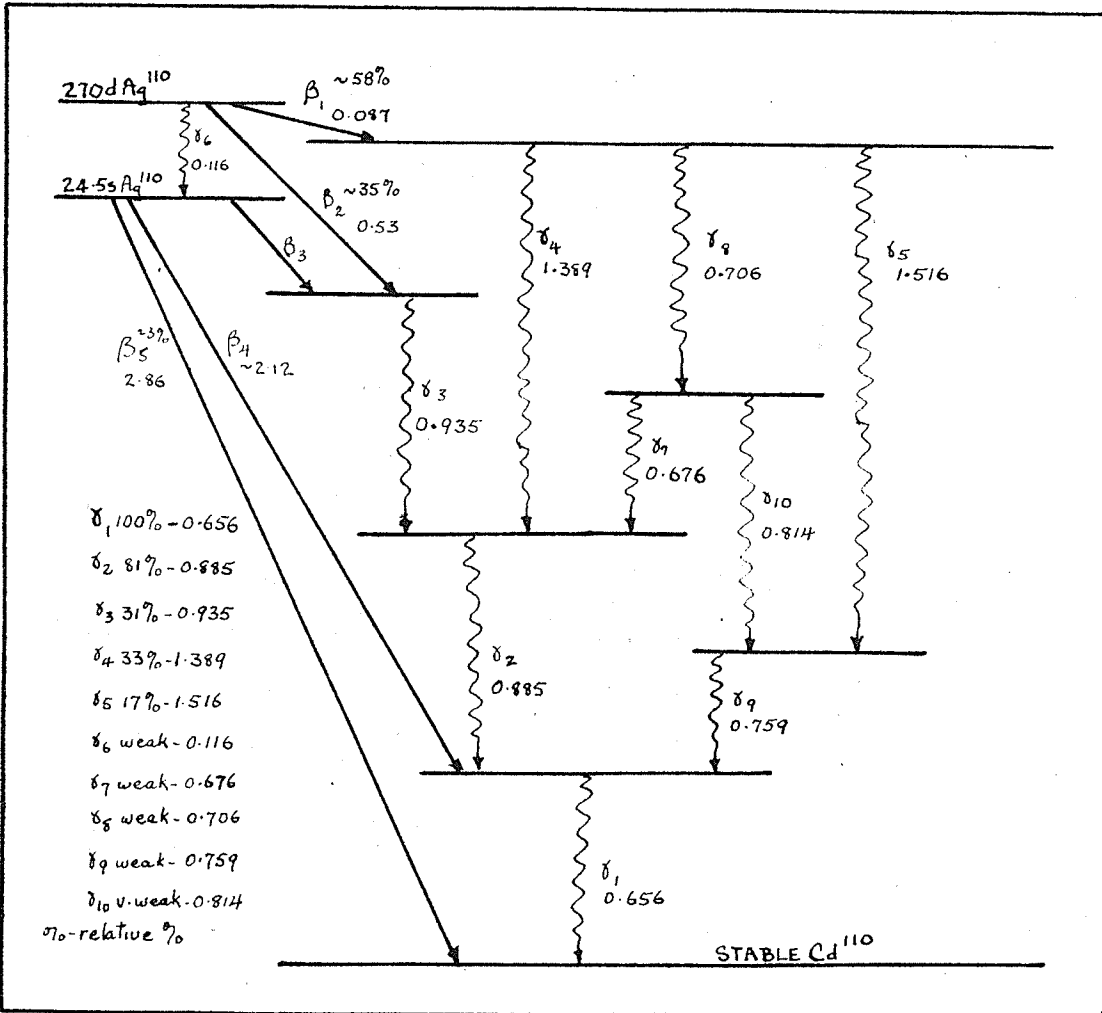


FIG. 13  
DECAY SCHEME OF  $\text{Ag}^{110}$

curves, drawn from the corrected number of activation counts are shown in fig. 14. It is obvious that the counting should have been taken over a longer period of time. This was done at a later date, and the decay curve obtained is shown in fig. 15. It is observed that there is only a slight change in the shape of the graph.

The graphs indicate the presence of two isotopes, one with a very short half life, and the other with a very long half life. The short half life is about 45 sec. and is due to  $\text{Ag}^{110}$ . The longer half life value, too long to be calculated from the graph, is most likely the 270 day half life associated with the  $\text{Ag}^{110}$  isotope. The numbers of 'initial' activation counts per two minutes, were found to be 65,000, 32,000 and 46,000 for E27-3, E27-2 and E27-1 respectively.

The assays originally obtained on these samples were;

E27-3.....10,834 oz. per ton, silver.  
 E27-2..... 7,373 oz. per ton, silver.  
 E27-1..... 7,313 oz. per ton, silver.

Assuming that the number of counts per two minutes of the silver sample. E27-3 was correct, then by simple proportion the other samples should have  $\frac{32,000}{1} \times \frac{10,834}{65,000}$  or 5,333 oz.

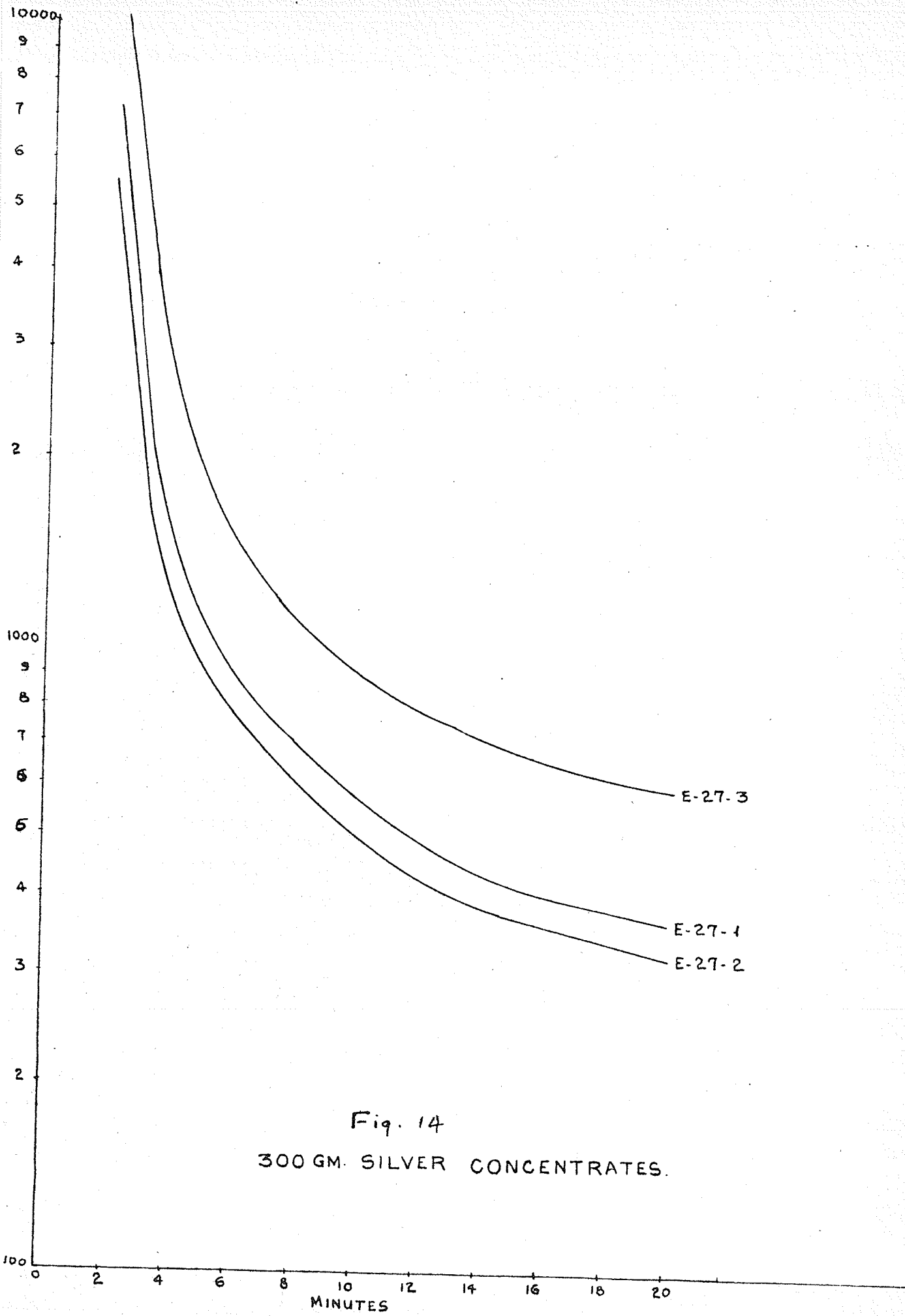


Fig. 14  
300 GM. SILVER CONCENTRATES.

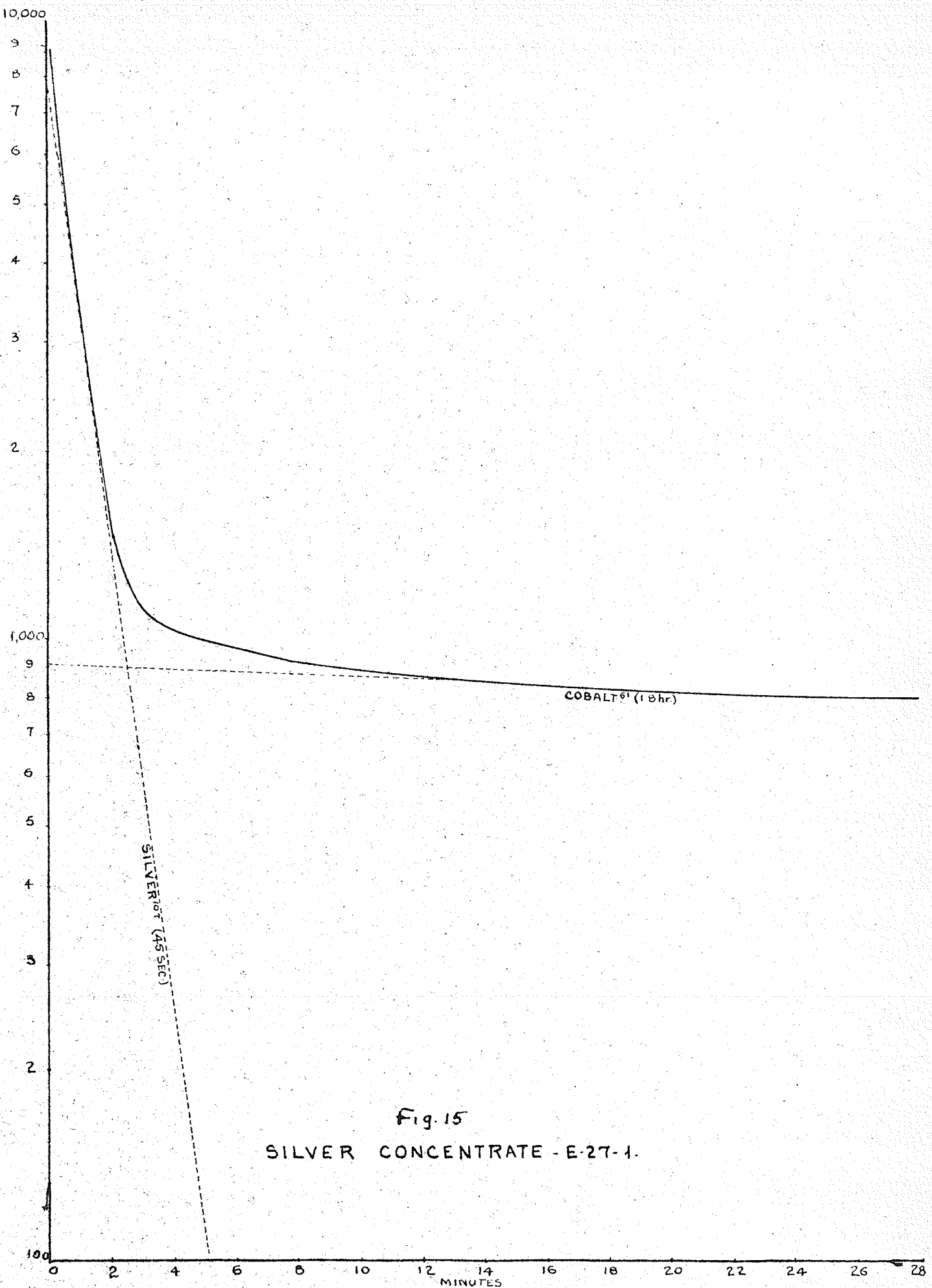


Fig. 15  
SILVER CONCENTRATE - E-27-1.

per ton for E27-2 and 7,666 oz. per ton for E27-1. There seems to be an error in either the assay values or in the values obtained in this experiment. Sample E27-2 was sent to the Mines Branch, Winnipeg, and an assay of 5,225 oz. per ton, silver and 1.93% cobalt was obtained. This result was more consistent with the results obtained in the laboratory.

It would be interesting to determine the amount of silver which could be detected in a rock sample. However, this could be done accurately, only when the apparatus is moved to a new location where the background counting rate would be appreciably lower than the present rate of +1000 counts per minute.

## MANGANESE.

The average manganese content of the lithosphere is 0.09%, and thus economical deposits are rare. A manganese concentration must contain at least 35% manganese to be considered an ore (19).

Manganese is the Achilles heel of the steel industry. Of all the metals used in making ferro-alloys, manganese is the most essential one. Sound steel cannot be produced without the use of a small amount of manganese to remove the oxide formed by melting the iron. It is also used as a desulphurizing agent.

In its natural form, manganese occurs solely as  $Mn^{55}$ . The cross section for thermal neutrons is 13.0 barns, and upon irradiation,  $Mn^{56}$  is produced. This isotope has a half life of 2.59 hours and decays either by a  $\beta^-$  emission (15%) of 0.73 mev., followed by two  $\gamma$  emissions of 2.13 and 0.845 mev., or by a  $\beta^-$  emission (25%) followed by  $\gamma$  emissions of 1.81 and 0.845 mev, or by  $\beta^-$  emission (60%) followed by  $\gamma$  emission of 0.845 mev. The relative percentages of the  $\gamma$  ray emissions are 2.13 mev., 12.5%; 1.81 mev., 18.75%; and 0.845 mev. 68.75%. Most of the counts, therefore will be those from the 0.845 mev.  $\gamma$  ray, and a photograph of the spectrum should clearly define this line.  $Mn^{56}$  decays to produce stable  $Fe^{56}$ .



The manganese ore used in this experiment was assayed by the Mines Branch, Winnipeg, at 54.4% manganese. A sample of 300 grams of the ore was activated for 20 minutes, and the experimental procedure followed was the same as that for the aluminum sample. Counts were taken at four minute intervals and the decay curve obtained is shown in fig. 16. A photograph of the activated sample was also taken and is shown in fig. 18a. The exposure time for the photograph was one hour.

To determine the percentage of manganese detectable, varying amounts were mixed with limestone. Limestone was chosen because experiments proved that the activity after irradiation was very small. The limestone used in the mixture was activated for 20 minutes, and the activation counts recorded. Mixtures of 10 gm. manganese ore and 390 gm. limestone, 5 gm. manganese ore and 395 gm. limestone and 2 gm. manganese ore and 398 gm limestone were activated for 20 minutes. The background counts which included the counts from the activated limestone and sample container, were subtracted from the reading obtained from the activated mixtures, and the results are shown in fig. 17. Photographs of the spectra were also taken and are shown in fig. 17,b and c.

From fig. 16, it is seen that the half life of the

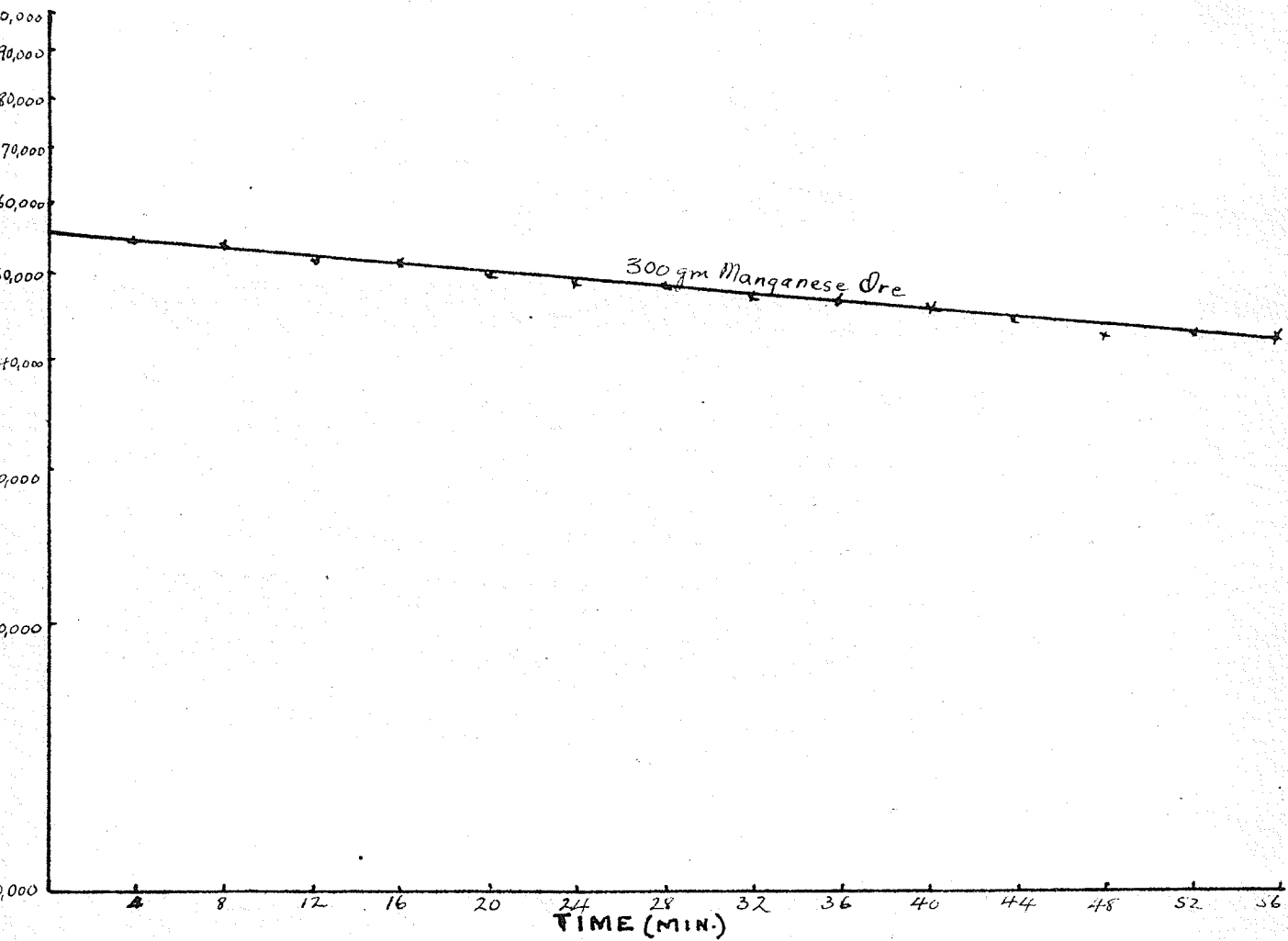


FIG 16

DECAY CURVE FOR ACTIVATED MANGANESE ORE.

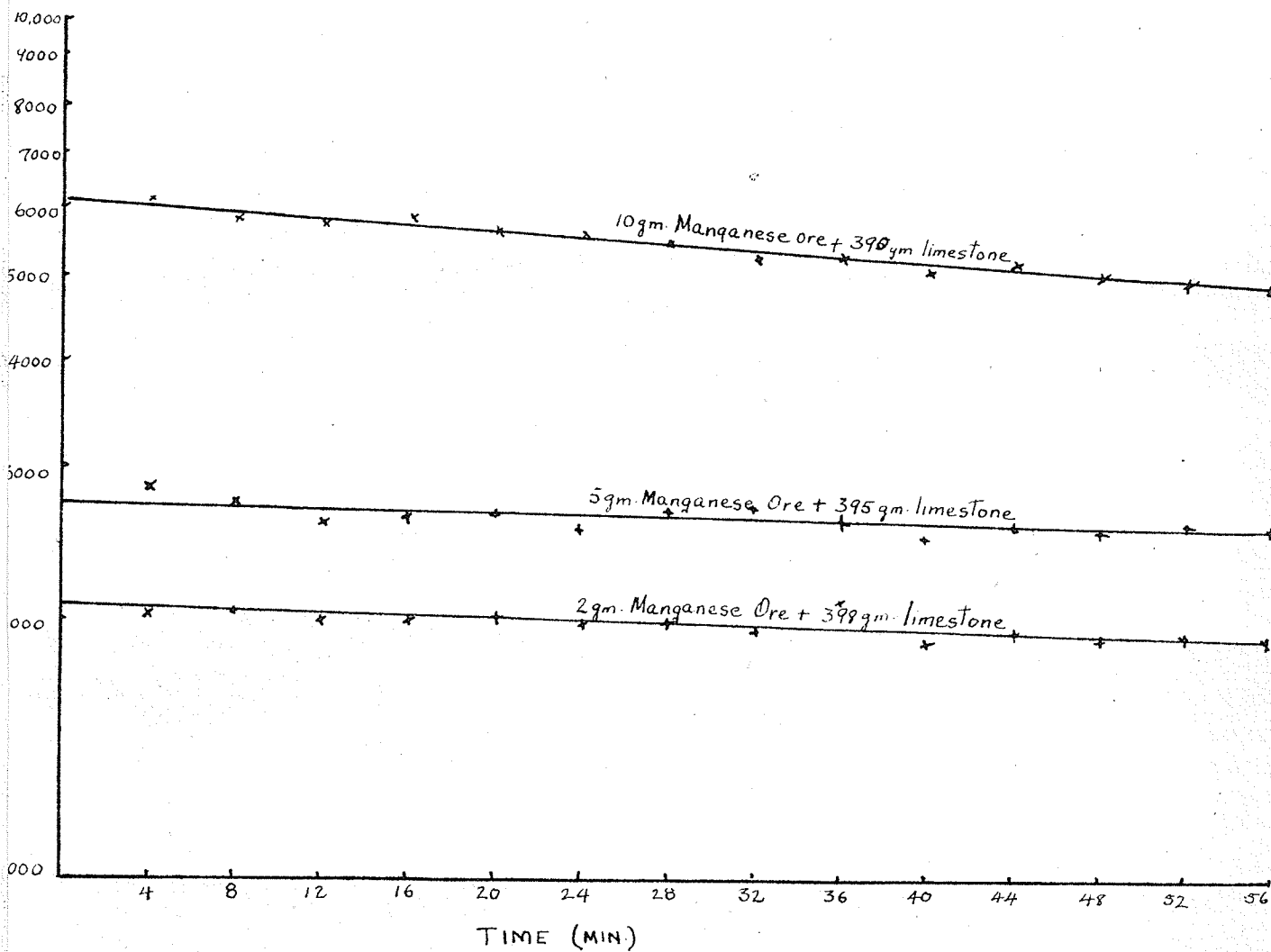


FIG 17

DETERMINATION OF MANGANESE CONTENT DETECTABLE

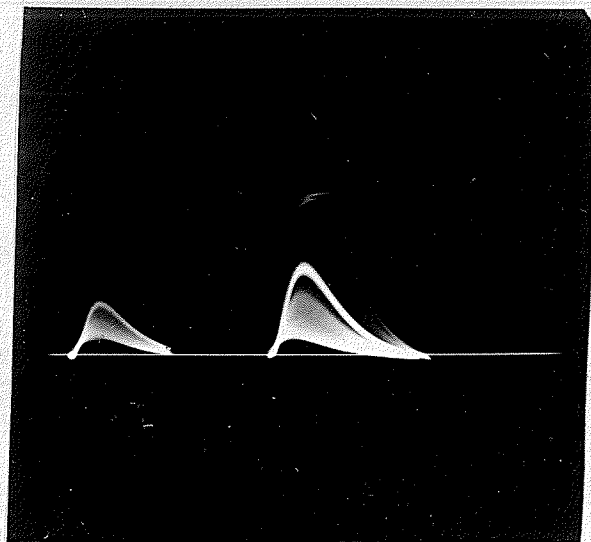
activated manganese is very long. A rough estimate is a value of about 4 hours. Although this sample had impurities, the activation counting rates from these were small compared to that of the manganese, and thus did not show up on the decay curve. For example, if there were 1000 initial counts from the activated impurities in the ore, the graph would have changed only very slightly. The 'initial' number of counts from the manganese (140 gm Mn.) was 14,250 counts per minute.

The photograph of the spectrum of the activated manganese ore shown in fig. 18a shows quite clearly the 0.845 and the 1.81 mev. energy lines. The Cs<sup>137</sup> calibration line is shown on the left of the manganese spectrum.

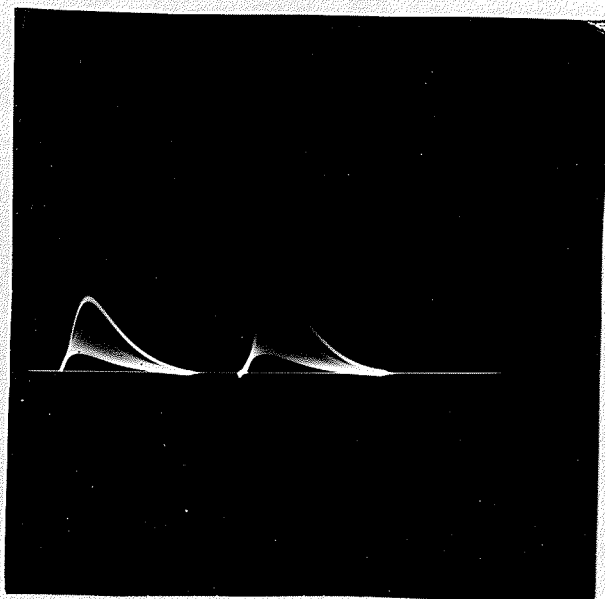
The determination of the manganese content detectable was carried out at a later date. Irradiation of 10 grams of manganese ore, ie. 5.4 grams of manganese, produced an 'initial' counting rate of 6,200 counts per 4 minutes, or 1,148 counts per 4 minutes per gram. Activation of 5 grams of the same ore, by simple proportion should give  $\frac{54.4 \times 5}{100}$  (1148), or 3,120 counts per 4 min. This agrees quite well with the 2,8000 'initial' activation counts obtained.

A 2 gram manganese ore mixture (1 gm. or 0.25% Mn), should

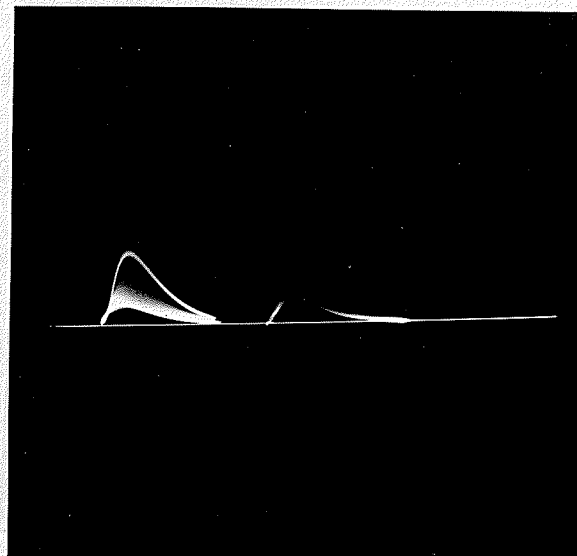
(65)



(a)



(b)



(c)

Fig. 18.

Spectra of Various amounts of Manganese Ore in Limestone  
 $\text{Cs}^{137}$  Spectrum on left of each photograph

- (a) 400 gm. Activated Manganese Ore
- (b) Activated Mixture of 10 gm. Manganese Ore in 390 gm Limestone
- (c) Activated Mixture of 5 gm. Manganese Ore in 395 gm Limestone

give by the same proportion, a counting rate of 1,148 counts per 4 minutes. However, the graphs shown in fig. 17 show a corrected activation counting rate of 2150 c/4 min. The error involved in the number of counts expected and the number found by experiment is due mainly to errors in weighing and to the high background. The samples used in previous experiments have all weighed 300 - 500 grams, and they were all weighed on a torsion balance. Weighing 2 grams of manganese ore was subject to a substantial percentage error.

The photographs shown in fig. 18 of the spectra of the various activated mixtures, all show the 0.845 mev. energy line from Mn<sup>56</sup>.

It is expected that with a lower background counting rate, more accurate results would be obtained from the 0.25% manganese mixture.

## COPPER

In its natural form, copper occurs as  $\text{Cu}^{63}$  (69.09%) and as  $\text{Cu}^{65}$  (30.91%).  $\text{Cu}^{63}$  has a cross section for thermal neutrons of 2.8 barns. Upon activation,  $\text{Cu}^{64}$  is produced, and this isotope decays by a  $\gamma$  emission of 1.34 mev., which follows a K capture process. There are other modes of decay, but these have no associated  $\gamma$  ray.  $\text{Cu}^{64}$  has a half life of 12.88 hours and decays to form stable  $\text{Ni}^{64}$ .

$\text{Cu}^{65}$ , the other form of natural copper, has a cross section for thermal neutrons of 2.1 barns, and upon activation forms  $\text{Cu}^{66}$ . This isotope has a half life of 4.34 minutes and decays by a  $\beta^-$  emission of 2.9 mev. and then by a  $\gamma$  ray emission of 1.32 mev.

Copper minerals, usually as mere grains, are present in all sorts of rocks and mineral veins. Zinc, lead, silver, and gold are the chief metals associated with copper deposits.

A sample of 340 grams of copper oxide,  $\text{CuO}$ , was irradiated for 4.5 min. This sample contains 271 grams of  $\text{Cu}^{63}$ . The number of counts per two minutes after activation were recorded, and after the necessary corrections were made, the graph shown in fig. 19 was drawn. A photograph of the spectrum was also taken. Another sample, weighing 500 grams

of copper ore was treated in a similar manner, and the decay curve and photograph of the spectrum obtained, are shown in fig. 19 and 20.

#### DISCUSSION

From the graph of the activated copper oxide shown in fig. 19, it is seen that the calculated half life is about 5.5 minutes. This differs from the reported half life of 4.34 minutes of the  $\text{Cu}^{66}$  isotope. This discrepancy is due to the fact that the curve was not taken for a long enough time, and the counts for the long life isotope were not obtained. Had this been done, the curve would have tapered off, and would have resulted in a component of the decay curve whose half life would have been less than the 5.5 minutes as calculated from the curve shown.

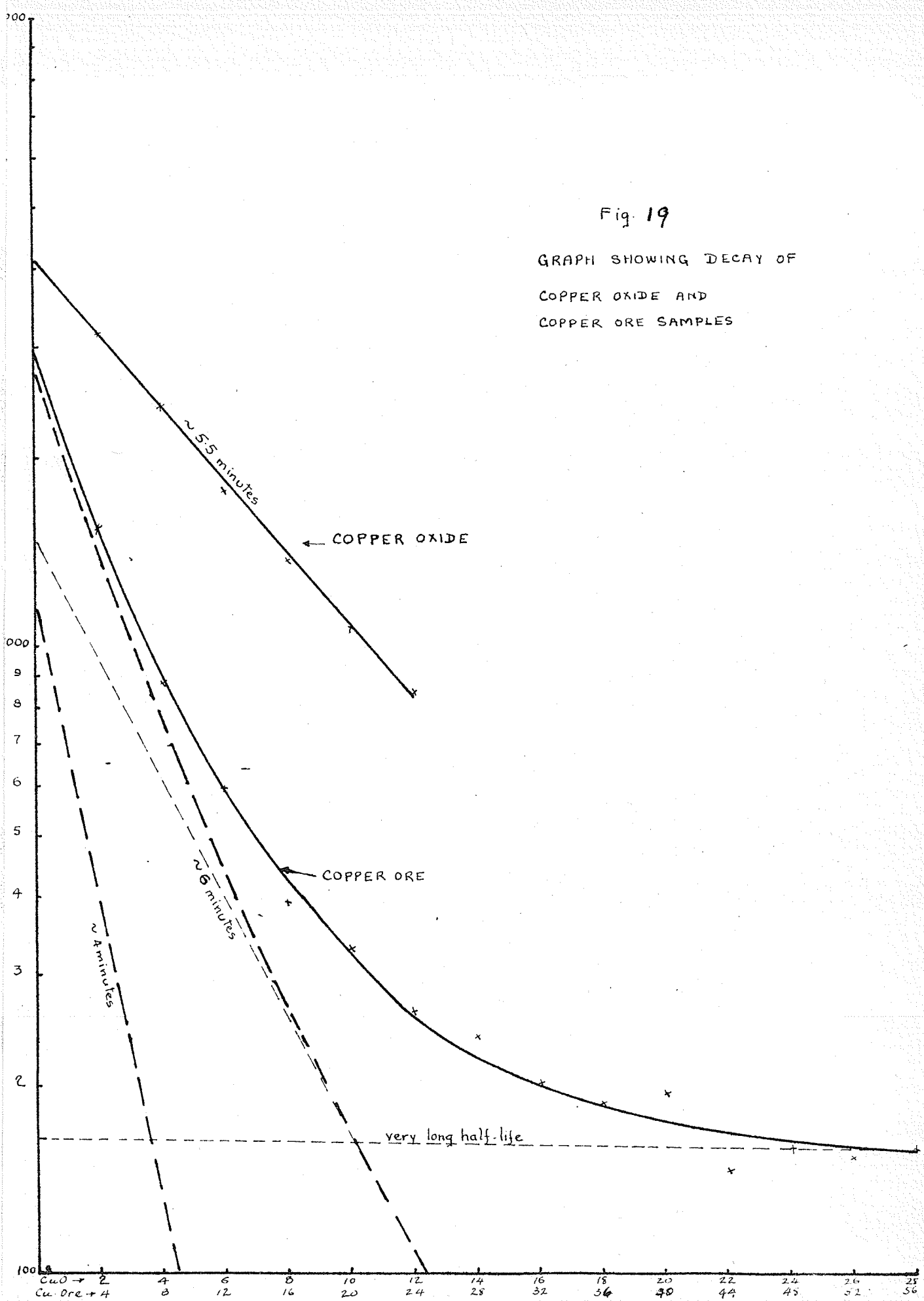
The shape of the graph showing the decay of the isotope produced by irradiating the copper ore, suggests the presence of three decaying isotopes. After resolving the curve into its composite parts, the calculated half lives were found to be 4 minutes, 6 minutes and a very long half life which is most probably due to the  $\text{Cu}^{64}$  isotope. The reported half life of this isotope is 12.88 hours.

The photograph of the spectrum shows three distinct lines. Although the spectrum is blocked on the scope, the



Fig. 19

GRAPH SHOWING DECAY OF  
COPPER OXIDE AND  
COPPER ORE SAMPLES



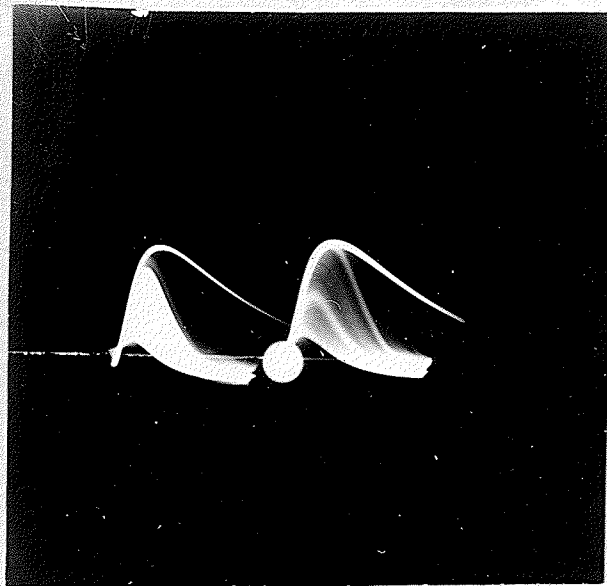


Fig. 20

Spectrum of Activated Copper Ore

Spectrum of Cs<sup>137</sup> on left

trailing edge of the 1.32 mev. line can be observed. There are also two very definite lines of lower energies. One occurs at an energy level of about 0.84 mev. This could be the  $\gamma$  ray emitted from the isotope  $\text{Ag}^{110}$ , which is produced when  $\text{Ag}^{109}$  (48.65%) is irradiated with thermal neutrons. The cross section for this reaction is 92 barns, and one of the reported  $\gamma$  rays emitted has an energy of 0.884 mev.

The other  $\gamma$  ray shown has an energy of about 0.4 mev. This could be due to traces of gold in the sample. Gold,  $\text{Au}^{197}$  (100%) has a cross section for thermal neutrons of 96 barns, and  $\text{Au}^{198}$  is produced by irradiation. This isotope emits a  $\gamma$  ray of 0.411 mev.

With a lower background counting rate, it seems quite possible that fairly low percentages of copper content could be analysed. It also seems possible to be able to make analyses on samples containing small quantities of silver and gold.

## MAGNESIUM

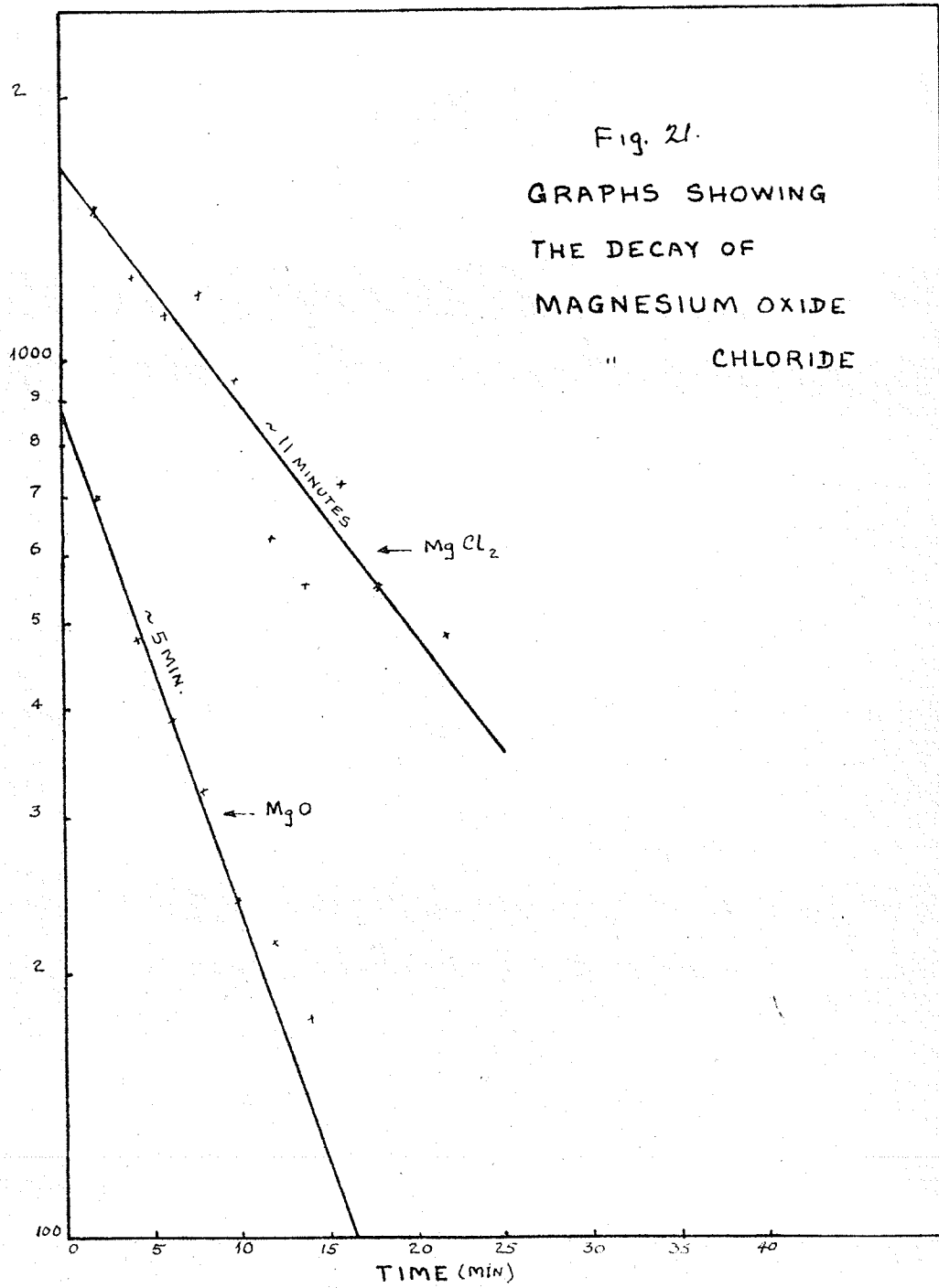
In its natural form, magnesium occurs as  $Mg^{24}$  79%,  $Mg^{25}$ -10%, and  $Mg^{26}$ -11%. Of these, only  $Mg^{26}$  has a cross section for thermal neutrons. Its value is 0.05 barns. Upon irradiation,  $Mg^{27}$  is formed and it has a half life of 10 minutes.  $Mg^{27}$  decays by a  $\beta^-$  emission (20%) of 0.7 mev., followed by two  $\gamma$  emissions of 1.01 and 0.84 mev. It also decays by a  $\beta^-$  emission of 1.8 mev. (80%), followed by a  $\gamma$  emission of 0.84 mev. The end product of the decay is stable  $Al^{27}$ . It is expected that the 0.84 mev. line would be the most intense line in the spectrum.

Two samples containing magnesium were tested. These experiments were performed solely to find the order of magnitude of the counting rate. The sample of magnesium chloride available weighed 135 grams. This was irradiated for ten minutes, and the decay curve obtained after activation, is shown in fig. 21.

The other sample used in this experiment was magnesium oxide. A sample of 400 grams was irradiated for 4.5 min. The decay curve is shown in fig. 21. A photograph of the spectrum was taken and is shown in fig. 22. The  $Cs^{137}$  calibration line is shown on the left.

The 'initial' activation counts, after the necessary

Fig. 21.  
GRAPHS SHOWING  
THE DECAY OF  
MAGNESIUM OXIDE  
" CHLORIDE



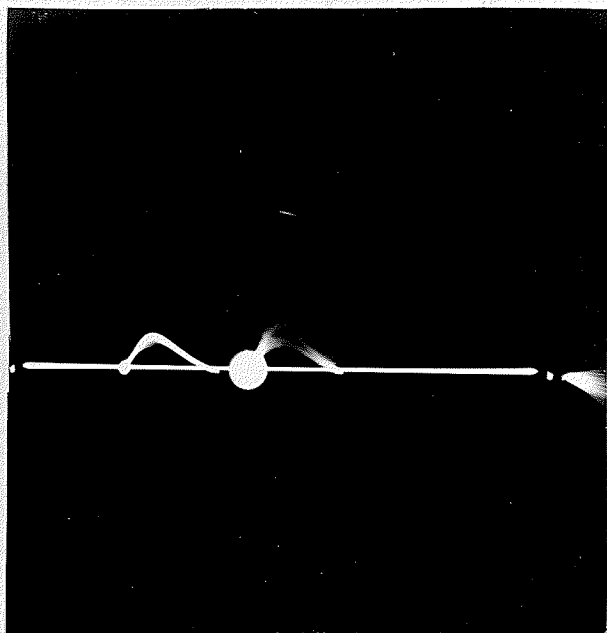


Fig. 22.

Spectrum of Activated Magnesium Oxide

Spectrum of Cs<sup>137</sup> on left.

corrections had been made, from the magnesium chloride was 1,720 counts per two minutes. The calculated half life was found to be about 11 minutes. This agrees with the reported value of 10 minutes for  $Mg^{27}$ . The 'initial' number of activation counts from the magnesium oxide, calculated from the decay curve, is 950 counts per two minutes.

The photograph of the spectrum of the activated sample of magnesium oxide shows energy lines of 0.821 and 1.20 mev. These energies agree with the values of 0.84 and 1.01 mev. expected from the  $\gamma$  rays from  $Mg^{27}$ .

The larger number of counts from the activated magnesium chloride sample is due to the activity from chlorine,  $Cl^{37}$ ., which has a cross section for thermal neutrons of 0.6 barns, and  $Cl^{38}$  which is formed after the irradiation. This isotope decays with  $\gamma$  emissions of 1.6 mev. and 2.15 mev.

If the counting rate was prolonged, this chlorine component would have been observed in the decay curve, and this would have made the calculated half life of the magnesium smaller, and more in agreement with the reported values.

## SANDSTONES, SHALES AND LIMESTONES

Any rock, having a sufficiently high porosity may serve as a reservoir for the accumulation of oil and gas (20). The most common one is sandstone, while others are limestone, dolomite, and shale. A study of these types of rocks was made, the object being to find if one type of rock could be differentiated from the other.

## SANDSTONES

Table 1 gives a chemical analysis of average sandstones. It is seen that 78.33% of this rock is  $\text{SiO}_2$  or quartz. The degree of cementation determines the softness and resistance of the rock, the cementing elements being chiefly silica, calcite (calcium carbonate) and iron oxides. Too much cement decreases the porosity of the rock and lessens the probability of the formation being a reservoir rock. An average porosity of 15% is generally used in computing possible production from oil sands.

The elements which are found in sands, and listed in table 1, would be activated in varying degrees when irradiated with thermal neutrons. The probable reactions are;

$\text{Al}^{27}$  (100%), (th n,  $\gamma$ ) 2.3 min.  $\text{Al}^{28}$ , 0.21 barns, 1.8mev.



|   |                        |
|---|------------------------|
| Si <sup>30</sup> (3.12%), (th n, $\gamma$ ) 2.7 hr. Si <sup>31</sup> , 0.12 barns         | ?                      |
| Ca <sup>48</sup> (0.18%), (th n, $\gamma$ ) 8.5min. Ca <sup>49</sup> , ----- "            | 2.7 mev.               |
| Ca <sup>44</sup> (2.13%), (th n, $\gamma$ ) 152days, Ca <sup>45</sup> , 0.66 "            | no rays.               |
| Na <sup>23</sup> (100%), (th n, $\gamma$ ) 14.9hr. Na <sup>24</sup> , 0.6 "               | 2.758mev.<br>1.380mev. |
| Fe <sup>58</sup> (0.33%), (th n, $\gamma$ ) 47days Fe <sup>59</sup> , 0.366 "             | 1.1, 1.3 mev.          |
| Mg <sup>26</sup> (10.97%), (th n, $\gamma$ ) 9.58min. Mg <sup>27</sup> , 0.05 "           | 1.01, 0.84,            |
| K <sup>39</sup> (93.08%), (th n, $\gamma$ ) 16x10 <sup>8</sup> y. K <sup>40</sup> , 3.0 " | 1.4 mev.               |
| K <sup>41</sup> (6.91%), (th n, $\gamma$ ) 12.4 hr. K <sup>42</sup> , 1.0 "               | 1.51mev.               |

The most probable of these, considering relative abundances of the isotope and the percentage of the element found in the rock are those involving Si<sup>30</sup> and Al<sup>27</sup>.

The sandstones were irradiated for 4.5 minutes, and then the activation counting rates were taken. The decay curves were drawn and from these, the 'initial' activation counts and the half lives of the isotopes produced upon activation were calculated. Photographs of the spectrum of these decaying isotopes were also taken.

Table 3 is a summary of the work done on sandstones.

Fig. 23 shows the decay curves of four samples from an oil well in Texas. Samples 1, 2 and 4 have similar decay curves, but sample 2, besides having a much higher counting rate than the other samples, has a complex decay curve. This suggests the presence of at least two isotopes. The

graphs of the decay of the other activated samples show the 2.3 minute half life due to the aluminum present in the sand. Fig.26, curve (b) shows another exception to the expected decay curve of a sand sample. The Lower Cretaceous Basal Quartz sand sample upon irradiation, gives a higher counting rate than expected, and has two half lives, the values of which are comparable to those found in sample #2 from the oil well in Texas.

The photographs shown in fig. 24 to 29, show very distinctly the 1.8 mev. energy line of  $Al^{28}$ . The  $Cs^{137}$  (665kev.) calibration spectrum is shown on the left of the pictures.

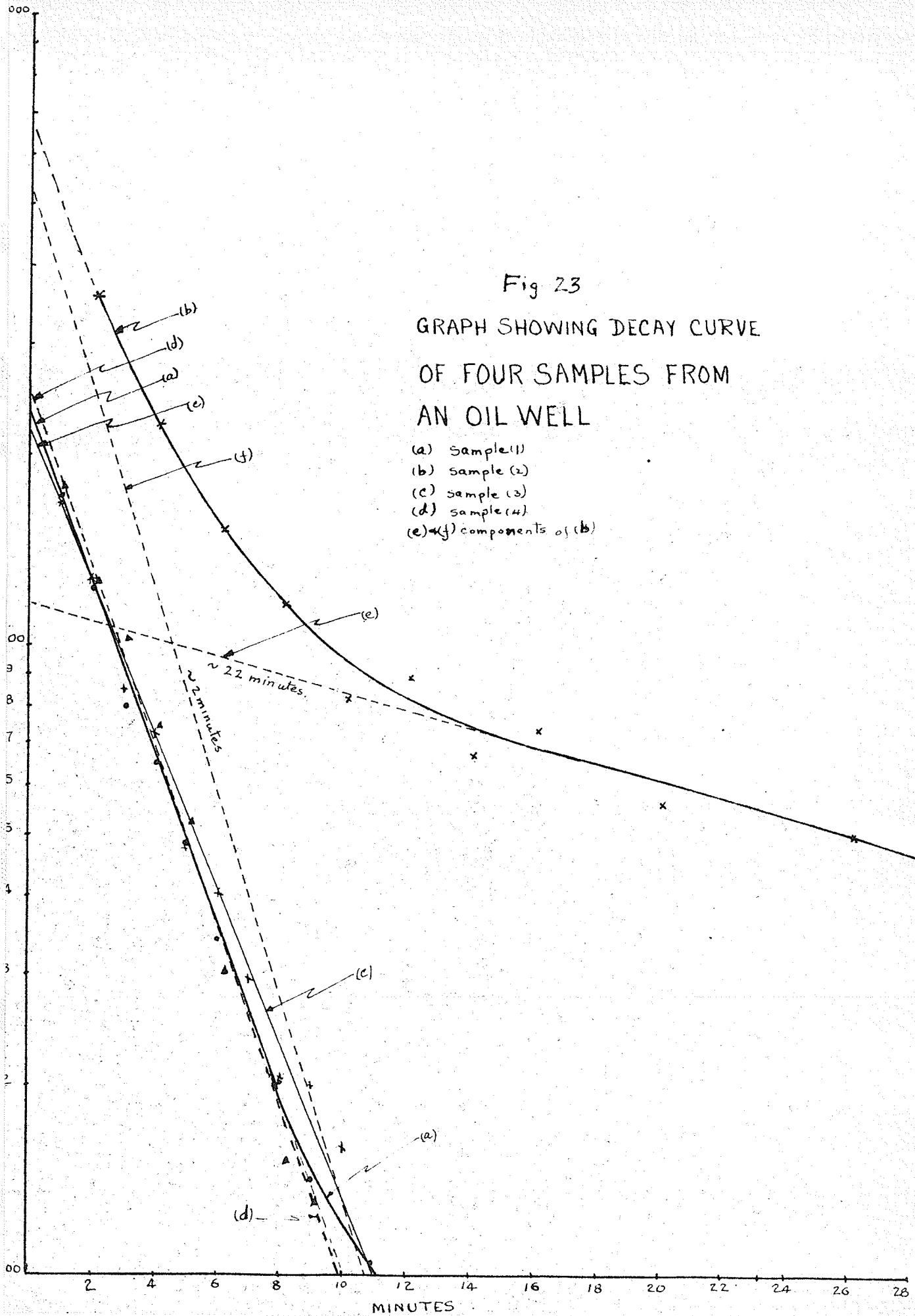
TABLE 3.

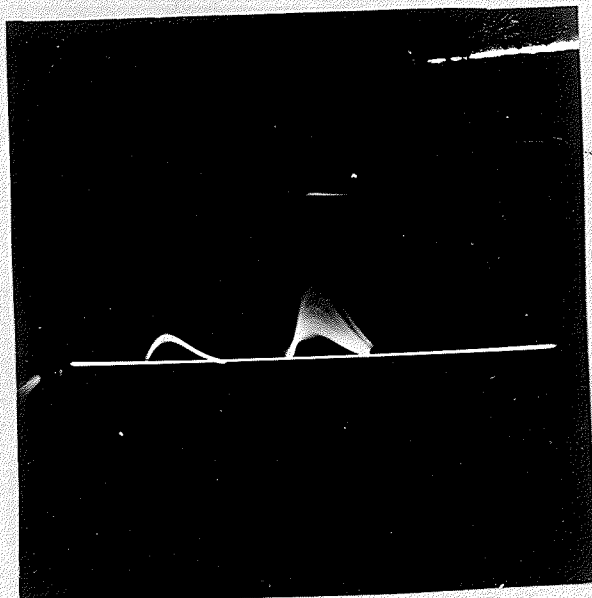
| SAMPLE                        | C/2m. | HALF LIFE | ELEMENT |
|-------------------------------|-------|-----------|---------|
| Sample #1, Texas Well         | 2,750 | 2.3m      | Al.     |
| Sample #2, Texas Well         | 6,810 | 2.0m      | Al.     |
|                               | 1,200 | 21.2m     |         |
| Sample #3, Texas Well         | 2,540 | 2.5m      | Al.     |
| Sample #4, Texas Well         | 3,000 | 3.0m      | Al.     |
| Lower Cretaceous Basal Quartz | 3,000 | 2.2m      | Al.     |
| Leduc Area                    | 395   | 13.0m     |         |
| Viking Sand                   | 1,320 | 2.4m      | Al.     |
| Non-productive Frio Sand      | 2,200 | 3.0m      | Al.     |
| Silica Sand-Black Island      | 1,370 | 3.0m      | Al.     |

Fig 23

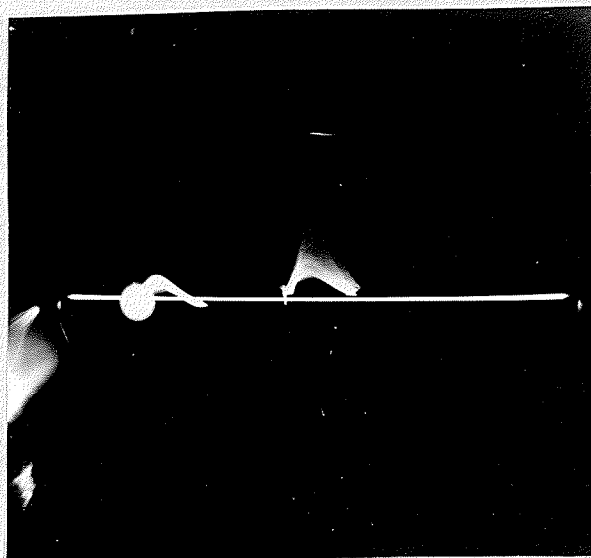
GRAPH SHOWING DECAY CURVE  
OF FOUR SAMPLES FROM  
AN OIL WELL

- (a) sample (1)
- (b) sample (2)
- (c) sample (3)
- (d) sample (4)
- (e) & (f) components of (b)

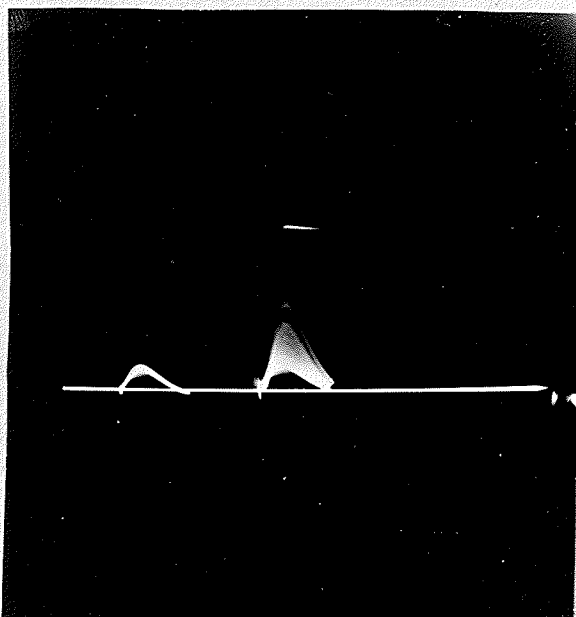




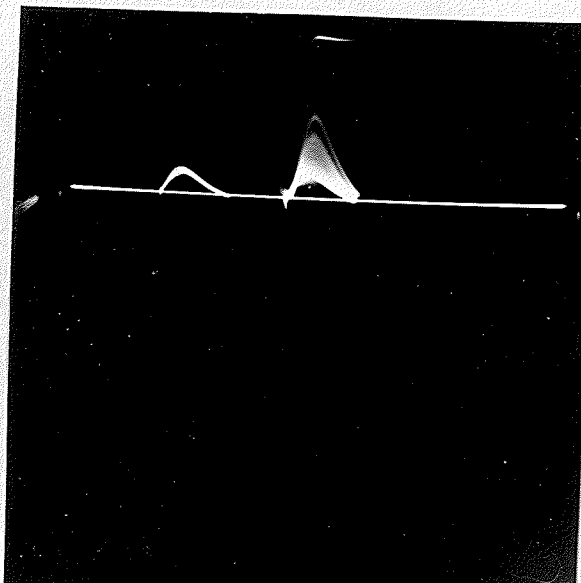
#1



#2



#3



#4

Fig. 24.

Spectra of Activated Oil Sand Samples from Texas Well

(Samples taken at different depths in drill hole)

Cs<sup>137</sup> Spectrum on left of photographs.

Fig. 25  
DECAY CURVES OF  
(a) activated Viking Sand.  
(b) " Black Island Sand.

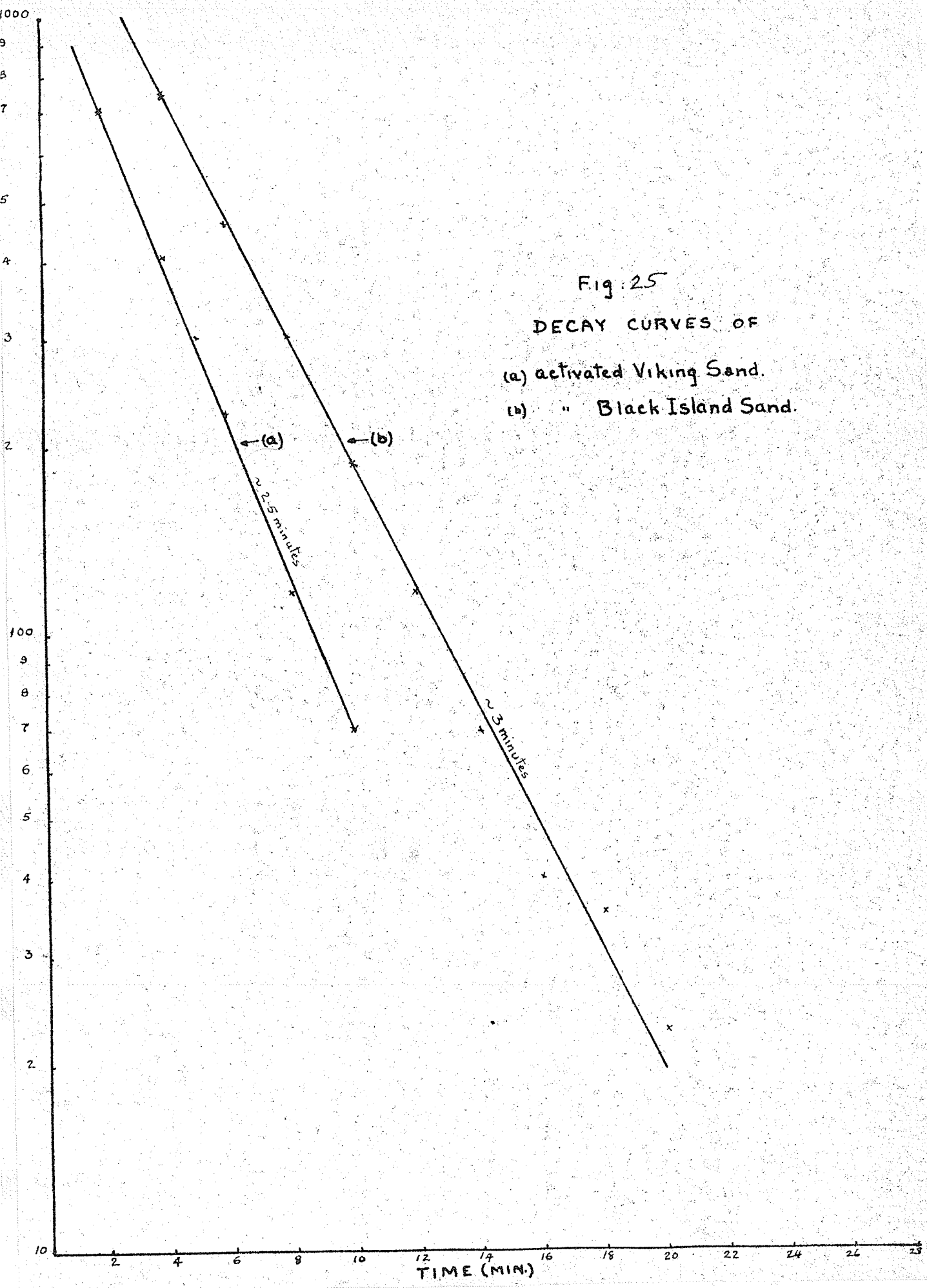
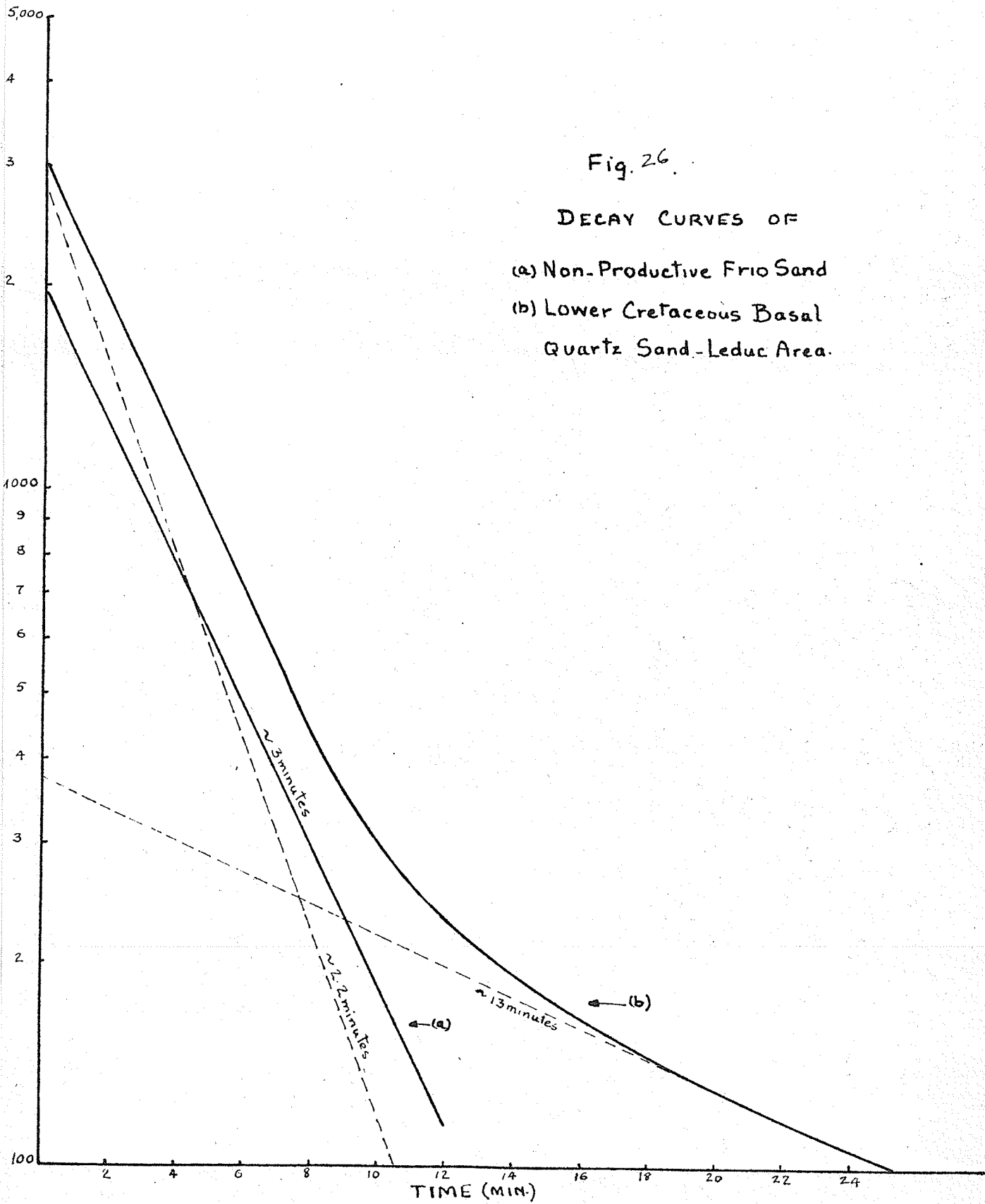


Fig. 26.

DECAY CURVES OF  
(a) Non-Productive Frio Sand  
(b) Lower Cretaceous Basal  
Quartz Sand-Leduc Area.



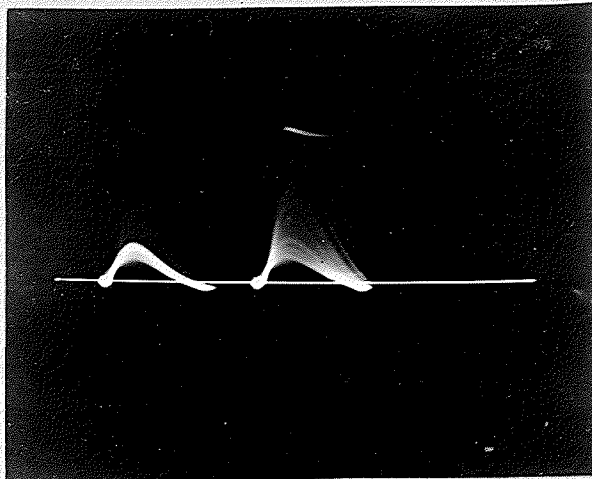


Fig. 27.  
Lower cretaceous Basal Quartz Sand  
Cs<sup>137</sup> on left

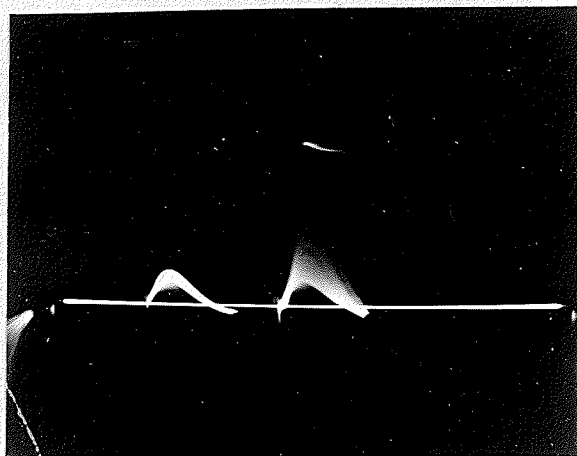


Fig. 28.  
Viking Sand  
Cs<sup>137</sup> on left

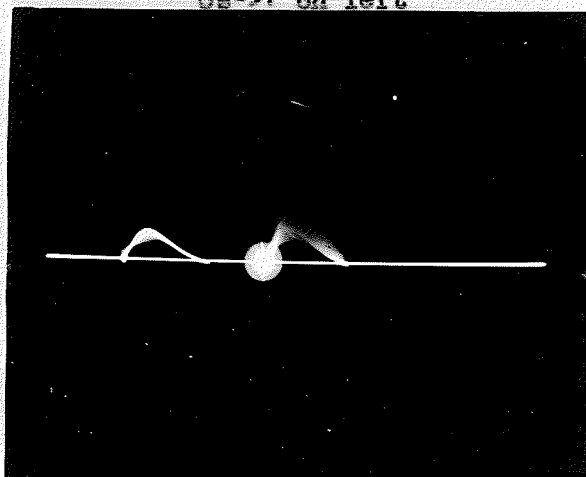


Fig. 29.  
Silica Sand  
Cs<sup>137</sup> on left

## SHALES

Shale is an impervious rock. It is sometimes sandy, and thus is more porous. A very hard shale, if not too deeply buried, might be fractured and retain the opening. A group of these openings, intersecting each other, might act as a reservoir for the collection of oil (20).

Table 1 shows the chemical composition of average shales. It is noted that the aluminum content of shales is greater than that of average sands. It is therefore expected that the counting rate of activated samples of shales would be generally higher than that of sands. Table 1 shows that the activation counts would be obtained principally from the isotopes produced from silicon and aluminum.

The same experimental procedure followed for the sand samples were followed for the shales.

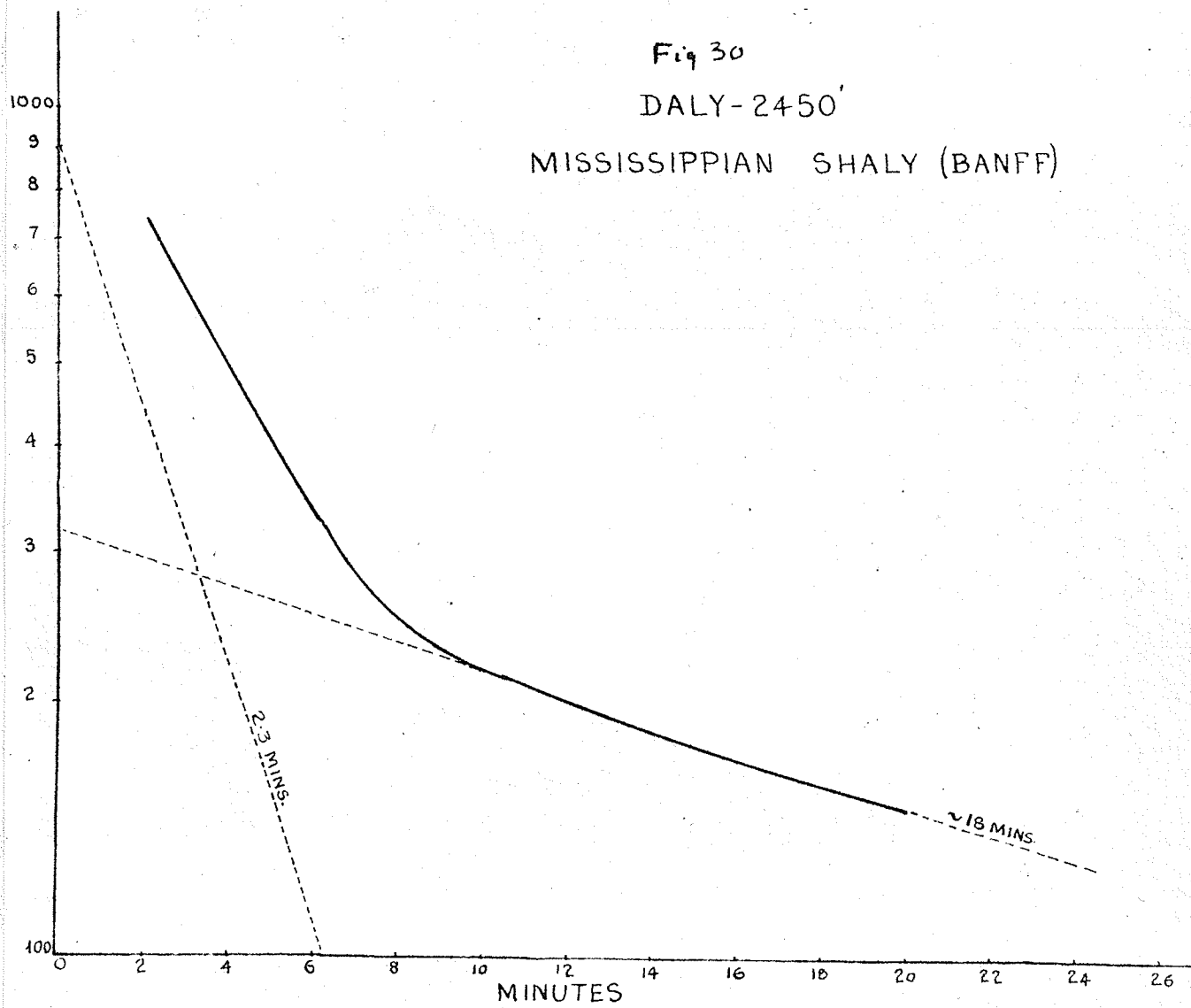
Table 4 is a summary of the results obtained. The most striking feature of the decay curves shown in fig. 30 to 32 is the presence of more than one decaying isotope. The photographs, shown in fig. 33 to 34 of the spectrum of the activated samples, all show very plainly, the 1.8 mev. energy line of  $Al^{28}$ . The  $Cs^{137}$  line is shown on the left of the pictures.



Fig 30

DALY-2450'

MISSISSIPPIAN SHALY (BANFF)



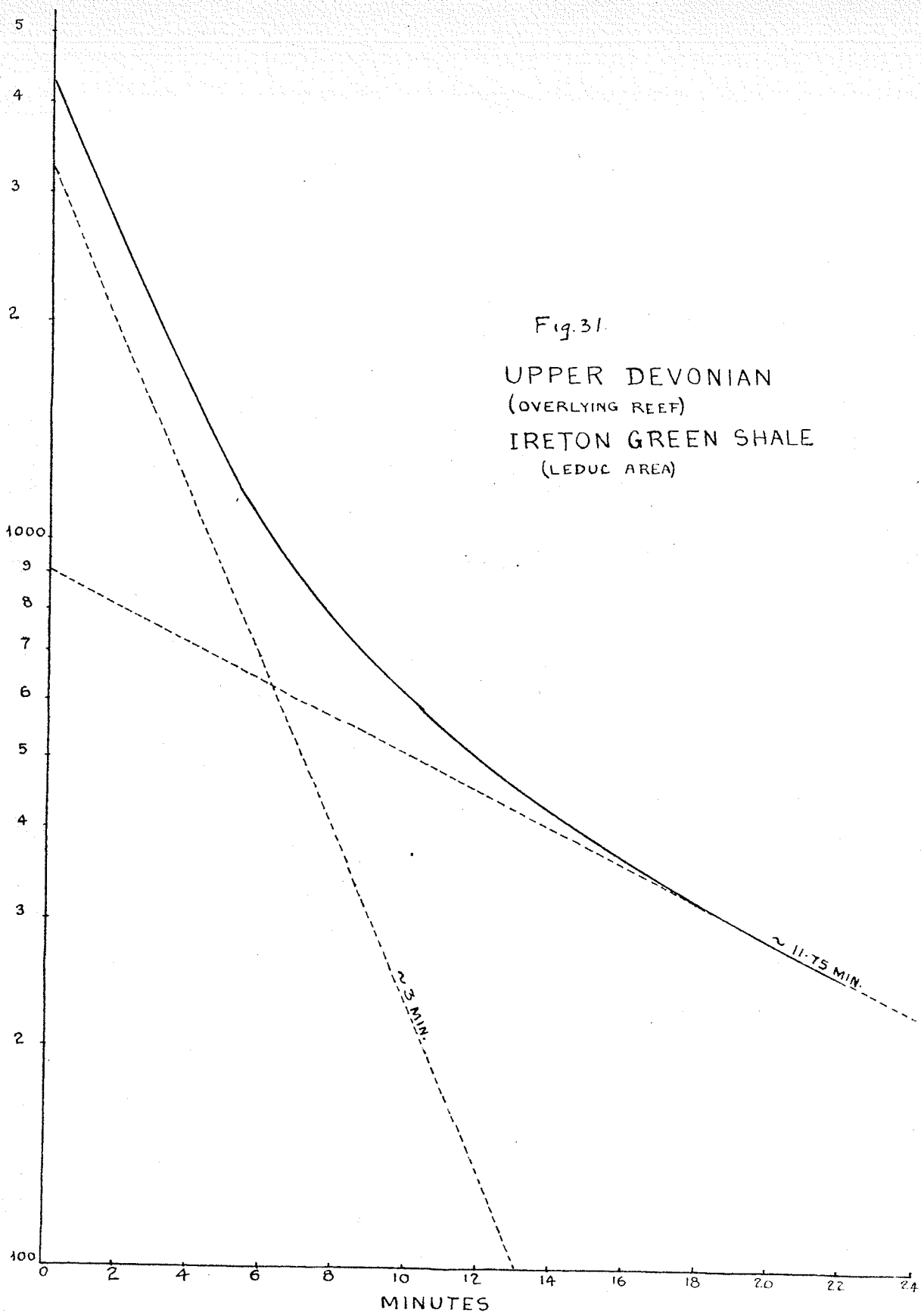


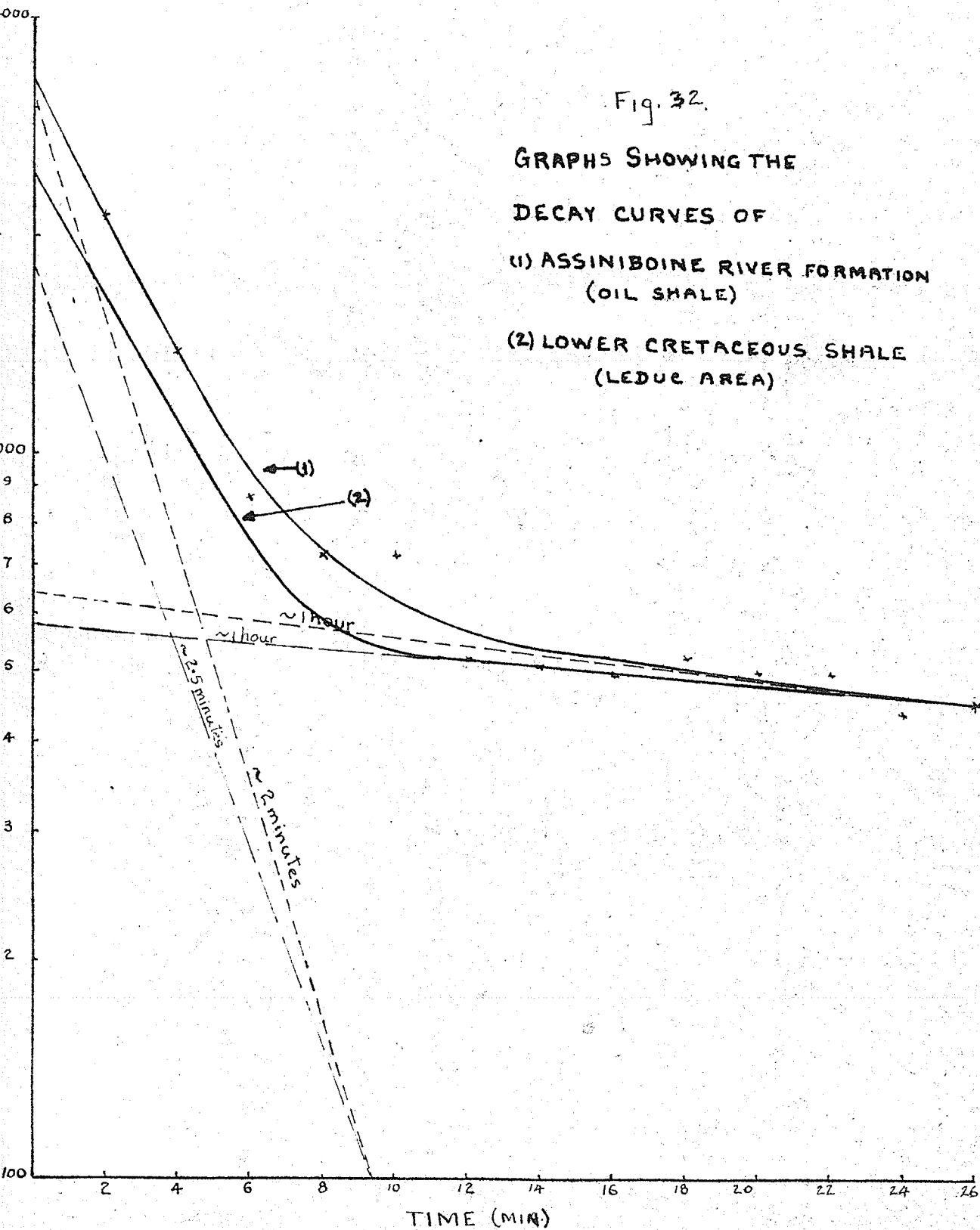
Fig. 32.

GRAPHS SHOWING THE

DECAY CURVES OF

(1) ASSINIBOINE RIVER FORMATION  
(OIL SHALE)

(2) LOWER CRETACEOUS SHALE  
(LEDUC AREA)



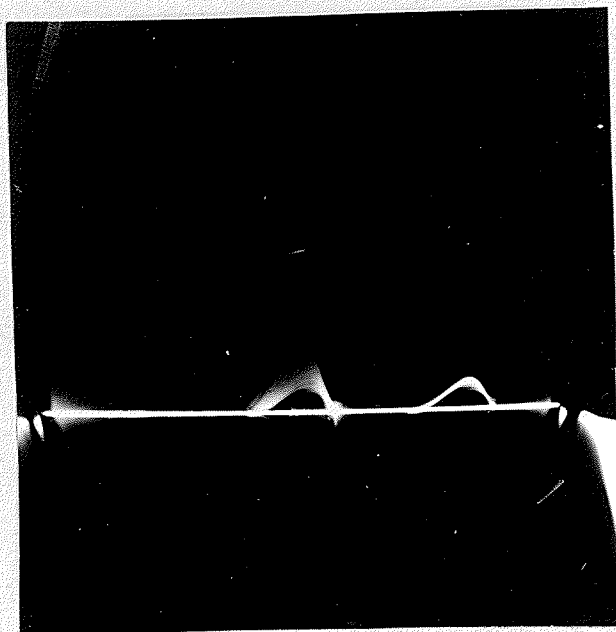


Fig. 33.  
Assiniboine River Formation  
(oil shale)  
Cs<sup>137</sup> on right

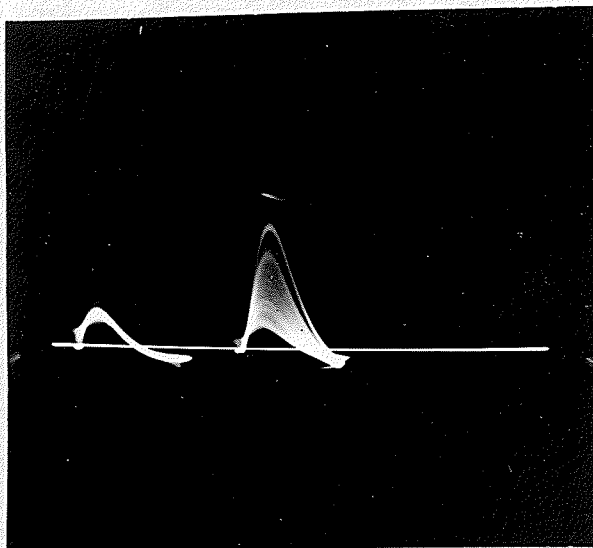


Fig. 34.  
Lower cretaceous shale  
Cs<sup>137</sup> on left

TABLE 4.

| SAMPLE                                     | G/2min.      | HALF<br>LIFE   | ELEMENT |
|--|--------------|----------------|---------|
| Upper Devonian Ireton Green<br>Shale       | 3,710<br>920 | 3.0m<br>11.75m | Al.     |
| Daly 2450'- Mississippian                  | 1,025<br>325 | 2.3m<br>18.0m  | Al.     |
| Assiniboine River Formation<br>(oil shale) | 3,810<br>650 | 2.0m<br>1.0h   | Al.     |
| Dower Cretaceous shale<br>(Leduc area)     | 1,950<br>590 | 2.5m<br>1.0h   | Al.     |
| Burning shale (Ontario)                    | 2,800<br>765 | 2.0m<br>26.0m  | Al.     |
| Waskeda, 3016, Jurassic Red<br>Beds        | 2,810<br>870 | 3.0m<br>29.5m  | Al.     |

## LIMESTONES

Although limestones are not very porous, yet a surprisingly large number of oil fields have been developed in this type of formation. Limestones make excellent reservoirs when they are fissured or channeled. Due to the solubility of these rocks, openings in them may be readily widened by water action, developing excellent cavities in which oil may accumulate. Coral reefs in limestone are important reservoirs.

Table 1 shows the chemical analysis of average lime-

stones. The obvious differences in the composition between limestones as compared to shales and sands are the smaller percentages of silicon and aluminum and the greater percentage of calcium oxide and carbon dioxide. It is plain that, since the relative abundance of the calcium which could be activated ( $\text{Ca}^{44}$ ) is only 2.13% and the cross section for thermal neutrons of calcium is small (0.61), the number of counts obtained after the irradiation of a limestone sample would be small.

Several samples were activated. The same experimental procedure followed with the samples of sands and shales, were followed with the limestones.

Table 5 is a summary of the results obtained.

TABLE 5

| SAMPLE                             | CPM ABOVE BACKGROUND |
|------------------------------------|----------------------|
| Samples 38,51,70 and 71 from Texas | 50,53,5 and 80 resp. |
| Mississippian Madison Limestone    | 380                  |
| Daly, 2403' - Mississippian        | 175                  |
| Waskeda- Jurassic lime             | 167                  |
| Wawanesa - Silurian                | 203                  |

The most interesting feature of the activation of the

limestone samples, as shown from the summary of the data obtained (table 5) is the very low induced radioactivity. It is seen that the number of counts were less than, or only slightly greater than 10% of the background counts. No accurate decay curves could be drawn as the number of actual counts were very small and thus the counting rate was erratic. No photographs were taken, as these would have only shown the background spectrum.

#### DISCUSSION

From the results obtained, it can be seen that to get accurate results from samples of shales, sands or limestones, activated or unactivated, the background counting rate would have to be made smaller. However, the results show that limestones can be easily differentiated from shales and sands by the very low counting rate, and that sands could be differentiated from shales by their lower number of activation counts and by their relatively simple decay curve.

Table 6 is a summary of the results obtained.

From table 1, it is seen that the  $Al_2O_3$  content in average shale is 15.4%; in average sand, 4.77%, and in average limestone, 0.81%. It would seem therefore, that the initial activation counts is an indication of the

aluminum content in the sample. Average shales have about 3 times as much aluminum as average sands, and it would be expected that the activation counts for shales would be about three times as high as the counts for sand samples. However, the sand samples were mostly oil sands, and this might be the reason for the high activity. Examining table 3, it is seen that the sand samples from the Texas well were all of a much higher activity than the sand samples which were not oil sands. Besides the higher activity, it can be seen from fig. 23 and fig. 25 that the oil sand decay curve is more complex than that of the average sand. In fact, the characteristics exhibited by the activated sand samples were similar in counting rate, shape of decay curve, and spectrum to the samples of activated shales.

TABLE 6

|   | SHALES              | SANDS                             | LIMESTONES           |
|---|---------------------|-----------------------------------|----------------------|
| Relative average Initial activation       | 100                 | 77                                | 8                    |
| Average half life as obtained from graphs | 2.3 min.            | Al. (1) 2.3m Al.<br>(2) long life | indefinite           |
| Spectrum on Oscilloscope                  | Distinct Al. Spect. | Distinct Al. Spect.               | no spect. available. |



## PRACTICAL APPLICATIONS OF ACTIVATION ANALYSIS

The striking feature of activation analysis is the comparatively short time necessary to produce results. This would suggest that the method would be useful in industry, especially where alloyed metals are manufactured. It is necessary to have repeated chemical analyses done on the alloy. In the steel industry, for example, the determination of the manganese percentage takes a few hours, while in the aluminum alloy industry an analysis of silicon and zinc requires a longer time. If the activation method of analysis is adopted, there would be a considerable saving of time.

Another very important aspect of activation analysis is the ease of preparation of the sample before analysis. It has been shown that it is not necessary to pulverize the rock samples. There is no need for the numerous amounts of chemical reactions or mechanical processes, which are so time consuming. This would be a great boon to industry, as many analyses could be made in a short time. Geologists who are interested in rock formation and who have to make numerous analyses of rocks over certain areas, would find this rapidity of analysis, a great advantage.

The scintillation counter can be used in determining

the formation of a drill hole. It has been shown that it is possible to differentiate between shales, sands and limestones. A drill, followed by a neutron source, and then by a sodium iodide crystal, shielded from the stray gamma rays, and a photomultiplier tube, with the other parts of the scintillation spectrometer on the surface, would form a much more accurate means of determining land formations than the Geiger Mueller tubes now used. The scintillation counter would thus be a fast and accurate method of determining land formation. This would be important in correlation of wells and the importance of this to oil logging is obvious.

The applications of this rapid and comparatively simple method of activation analysis are numerous and important in industry as well as academically. Experiments have yet to be done in developing methods for the analysis of elements to produce more accurate and consistent results.

## CONCLUSION.

The main purpose of this experiment was to determine the possibilities and limitations of the scintillation spectrometer in activation analysis.

The results obtained in the study of aluminum and manganese show that economical deposits of aluminum can be analysed quite accurately, and that manganese concentrations of about 0.5% could also be determined accurately. Taking into consideration the differences in flux, the amount of sample used, and the geometry of the apparatus, a comparison shows that the number of activation counts obtained during the experiments of aluminum and manganese were very much higher than the number obtained by Gaudin et. al. This is not really surprising, and is but another proof of the much higher efficiency of the scintillation counter as compared to the Geiger Mueller counter.

Of the elements tested, it is seen that activated aluminum, silver, and manganese gave activities which were at least four times the background counting rate, while calcium, iron and magnesium gave activities equal to or less than the background. Referring to table 2, it is seen that while the cross section for  $\text{Ca}^{44}$  (0.6 barns) is higher than that for  $\text{Al}^{27}$  (0.21 barns), the relative abundance of  $\text{Ca}^{44}$  is 2.13%, while that of  $\text{Al}^{27}$ , is 100%.  $\text{Al}^{27}$ ,  $\text{Ag}^{107}$ ,  $\text{Mn}^{55}$ , and  $\text{Cu}^{63}$  have relative abundances of 100%, 51.35%, 100%, and 69.09%

respectively, while  $\text{Ca}^{44}$ ,  $\text{Fe}^{54}$ , and  $\text{Mg}^{26}$  have relative abundances of 2.13%, 5.9%, and 11% respectively. The relative abundance is thus a very important factor in the number of activation counts. For those samples which gave low activation counts, it is suggested that a much larger sample, or a much higher neutron flux be used.

It would be necessary to perform experiments on a large number of elements, particularly those commonly found in rocks. These elements should be as pure as possible and could then be used as standards. The half lives and the initial activities, determined under known and reproducible conditions, i.e. amplification, discriminator bias settings, and voltage applied to the photomultiplier tube, should be compiled and used for reference.

There are many practical problems to be still solved. One of these concerns the time taken between the end of the irradiation period and the beginning of the counting process. It may be possible, by electronic or mechanical devices, to remove the sample from the plastic column and to place it on the crystal in less time than it now takes.

Another important consideration, especially in cases where the activation counting rate is small, is that of the neutron background counting rate. During the experiments, it was difficult to shield the crystal adequately from scattered

gamma rays, because there was not enough lead available.

More accurate results and a higher percentage determination of elements in rocks could be made if the background counting rate is made smaller.

## REFERENCES

1. Long, J.V.P. Brit. D.S.I.R. Report CRL/AE 60.
2. Gaudin, Sentfle and Freyberger Engineering and Mining Journal, 95, Nov.1952.
3. Pringle, Roulston, and Taylor Review Sci. Inst.,21,216(1950)
4. Jordan, W.H. Report on Scintillation Counter Symposium, 1949.
5. Pringle, R. W. Nature, 166,11 (1950).
6. Klein and Nishina Z. Physik, 52,853 (1929).
7. Halliday, D. Introductory Nuclear Physics, (John Wiley and Sons Inc. New York, 1950).
8. Devons, S. Excited States of Nuclei, (Cambridge University Press).
9. Breit and Wigner Phys. Rev. 49,519 (1936).
10. Kinsey, Bartholomew and Walker Phys. Rev. 83,520 (1951).
11. Sentfle and Leavitt Nucleonics 6,554 (1950).
12. Way, Fano, Scott and Thew NBS Circular 499 - Nuclear Data.
13. Tyrell, G. Principles of Petrology. Dutton and Co. New York, 1926.
14. Eicholz E.G. Topical Report, TR-93/51.
15. Roulston Nuclear Physics, Chicago University Press.
17. Tarr, W.A. Introductory Economic Geology McGraw Hill Book Co. Ltd. New York, 124,1930.
18. Lahee. Field Geology, McGraw Hill Book Co. New York, 1952.